THE EFFECT OF A STRONG MAGNETIC FIELD ON THE MOTT TRANSITION IN SEMICONDUCTORS

D. G. Hughes

A Thesis Submitted In Candidature for the
Degree of Master of Science

Department of Physics
Lakehead University
Thunder Bay, Ontario

July - 1970

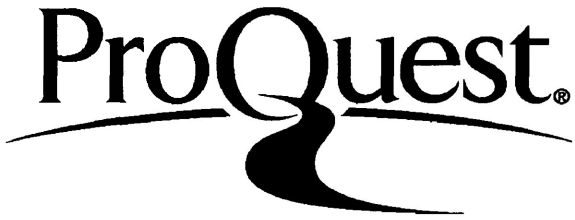

Abstract

This thesis considers the effect of a magnetic field on the transition from a conducting to a non-conducting state in impurity semiconductors, with particular reference to indium antimonide. Two models for such a transition have been proposed: one is based on the disappearance of bound states of the impurity due to screening by conduction electrons and the other is based on the onset of conduction due to overlap between the electron wave functions on adjacent impurity sites. The present work extends the latter model to include the effect of magnetic fields.

The theoretical work of Yafet, Keyes and Adams (Ref. 6), Fenton and Haering (Ref. 5) and Durkan and March (Ref. 10) is reviewed in Section 2 of the thesis. In Section 3 a dielectric approach to impurity conduction, due to Frood (Ref. 12), is introduced; he shows that the impurity system is non-conducting when $4\pi/3\epsilon_0 \, N\bar{\alpha} < 1$ where N is the impurity concentration, $\bar{\alpha}$ is the average polarizability of an impurity atom and ϵ_0 is the dielectric constant of the background crystal. We use this criterion in Section 4 to calculate a value of the critical magnetic field needed to make conduction cease, deriving $\bar{\alpha}$ as a function of magnetic field from a variational calculation of the ground state energy of the impurity. Our calculation is carried out for $T = 0^{\circ}K$, so that the impurities are all in the ground state and there are no elec-

trons in the conduction band (i.e. we do not consider excited states of the impurity or screening by conduction electrons). Finally we compare theoretical predictions with published experimental results.

Acknowledgements

I wish to express my gratitude to Dr. V. V. Paranjape for his guidance at all stages of the work presented in this thesis.

My thanks are also due to Dr. M. Kriechbaum for programming the numerical calculations.

TABLE OF CONTENTS

Abstract

Acknowledgements

Table of Contents

			PAGE
SECTION 1		The Basic Idea Underlying the Mott Transition	1-5
SECTION 2		The Effect of a Magnetic Field on Impurity Conduction	6-20
	2.1	The Work of Yafet, Keyes and Adams	6-10
	2.2	The Work of Fenton and Haering	11-13
	2.3	The Work of Durkan and March	14-20
SECTION 3		The Dielectric Approach to Impurity Conduction	21-30
	3.1	The Criterion for Impurity Conduction	21-24
	3.2	The Dielectric Constant of the Donors and Crystal	25-30
SECTION 4		Calculation of the Magnetic Field Required to Reverse the Mott Transition	31-53
	4.1	The Basic Model	31-32
	4.2	Calculation of the Polarizability	32-33
	4.3	Calculation of α_{11}	33-39
	4.4	Calculation of $\alpha_{\perp}$	39-41
	4.5	Numerical Calculations	42-44
	4.6	Discussion and Conclusions	45-53

REFERENCES

FIGURES

LIST OF SYMBOLS

SECTION I The Basic Idea Underlying the Mott Transition

The band theory of solids leads us to believe that when atoms are combined to form a crystal, the electron energy levels corresponding to the free atoms broaden into bands. To decide whether a given crystal will be an insulator or a conductor we recall that a Brillouin zone contains as many allowed $\underset{\sim}{k}$-vectors (i.e. distinct electron wave functions) as there are unit cells in the crystal. Allowing for spin, it follows that there are two electron states per unit cell in each band. Hence, a crystal with an odd number of free electrons per unit cell (e.g. the monovalent metals, the alkali metals) will have its topmost occupied band half-empty and the crystal will conduct. This simple application of band theory suggests that materials of the type referred to will behave as metals even if the atoms are very far apart. Though the bands may then be very narrow they will still be half-empty. That this is incorrect was first pointed out by Mott (Ref. 1), whose essential argument is as follows:

Consider an array of monovalent atoms. If an extra electron is added it can move freely through the lattice and its energies form a "conduction band". Similarly, if an electron is removed from one of the atoms then a mobile positive hole is formed. Suppose now we remove an electron from one atom (requiring an amount of energy I, the ionization energy) and place it on another atom (releasing an amount of energy E, the electron affinity). If

the atoms are very far apart the energy, W, needed to do this will be given by

$$W = I - E.$$

As the atoms are allowed to come closer to each other, W will decrease, but W cannot tend to zero since the hole and the electron attract each other with a Coulomb force and it is known (Ref. 2) that such a force leads to bound states; the oppositely charged carriers in fact form a bound pair and even if they move through the lattice will do so as a pair without producing any net current. One can imagine a small number of such pairs being formed (the meaning of "small" will be discussed in a moment); the above reasoning is unchanged and the material remains non-conducting. Suppose, however, that a large number of pairs have been formed and we now form one more. The electron we remove will no longer move in a Coulomb potential but, owing to the electrons already displaced, in a screened potential of the form (Ref. 3)

$$-\frac{e^2}{r}\exp(-\lambda r)$$

in which e, r have their usual meaning and $1/\lambda$ is the screening length, which will depend on the concentration of displaced electrons. Such a potential does not necessarily lead to bound states and the electron (and all subsequent ones removed) may be free to

carry current.

Mott's argument, then, leads to the view that the number of free carriers may be large or it may be zero; it cannot be small. The transition from a non-conducting to a conducting state will be a sudden one, occuring at some critical value of the atomic spacing.

In fact, as Ziman points out (Ref. 4), if the screening length, $1/\lambda$, is less than the ground state radius of the atom even this state cannot be bound and he uses this as follows to estimate the critical spacing at which the transition occurs. Assuming that the atoms are hydrogen-like, the ground state radius, a_H, is given by

$$a_H = \frac{\hbar^2}{me^2} \tag{1.1}$$

with the usual symbols, and λ is given by

$$\lambda^2 = \frac{4me^2}{\hbar^2} \; n^{1/3} \tag{1.2}$$

where n is the number density of ionized electrons.

Hence

$$\lambda^2 = \frac{4}{a_H} n^{1/3} \tag{1.3}$$

The system will conduct if $\frac{1}{\lambda} < a_H$

i.e. if $\lambda^2 > \frac{1}{a_H^2}$

Using (1.3) this condition becomes

$$\frac{4}{a_H} n^{1/3} > \frac{1}{a_H^2}$$

or

$$n^{-1/3} < 4a_H \qquad (1.4)$$

i.e. the system will conduct if the average spacing between atoms is less than four atomic units.

In his paper, Mott applies the above theory to impurity band conduction in semiconductors by treating the impurities as hydrogen-like centers in a medium of dielectric constant ε_o, the dielectric constant of the background crystal; the mass, m, of the electrons is replaced by m^*, the effective mass and the charge, e, is replaced by $e/\sqrt{\varepsilon_o}$.

On this basis, the critical concentration for donor impurities in silicon, for example, taking $m^* = 0.45m$ and $\varepsilon_o = 12$, is about $10^{19}cm^{-3}$, using the criterion of (1.4). This agrees with the value given in Table I of Ref. 1. For indium antimonide the critical concentration of donors given by (1.4) is, taking $m^* = 0.01m$ and $\varepsilon_o = 16$ (as in Ref. 5), about $4 \times 10^{13}cm^{-3}$. As Ziman points out, the numerical factor on the right-hand side of (1.4) need not be taken too seriously; in a crude way one could argue that the transition will take place when the overlap between neighbouring

impurities is sufficiently strong, when they are, say, one Bohr radius apart. In In Sb this argument would lead to a critical concentration of about $2 \times 10^{15} cm^{-3}$. It will be of interest to compare these estimates with the figures calculated on a different basis for In Sb in the latter part of this paper.

SECTION 2 The Effect of a Magnetic Field on Impurity Conduction.

2.1 The Work of Yafet, Keyes and Adams.

We now ask what effect a magnetic field will have on the Mott transition. Since we are going to treat impurity conduction on the basis of hydrogen-like impurities embedded in a background dielectric medium it is clearly relevant to ask what effect a magnetic field has on a hydrogen atom; this problem has been considered by Yafet, Keyes and Adams (Ref. 6).

They present their results in terms of a dimensionless parameter, γ, defined by

$$\gamma = \frac{\hbar\omega_c}{2R_y} \tag{2.1}$$

where ω_c is the cyclotron frequency of a free carrier in the magnetic field and R_y is the Rydberg. γ is, in fact, the ratio of $\hbar\omega_c/2$, the zero point energy of a free carrier in a magnetic field, to R_y, the energy of a carrier in the lowest state of the hydrogen atom in a field-free region. Yafet, Keyes and Adams point out that if $\gamma<<1$ (the magnitude of the magnetic field required for this to be so will be discussed below) then the magnetic forces on the electron are not comparable to the Coulomb forces; for $\gamma>1$, however, the magnetic forces, which are centripetal in a plane perpendicular to the field, B, will compress the atom and this will result in an increase in the magnitude of the (negative) Coulomb energy. On the

band model of a semiconductor this means that the impurity level is lowered with respect to the bottom of the conduction band; in other words, the binding energy of the impurity increases with magnetic field. It is with this latter effect that Yafet et al are chiefly concerned. It should be clear, however, that the shrinkage of the atom in a strong magnetic field will result in a decrease of the overlap between neighbouring impurities and hence in an increase of the critical concentration at which the Mott transition occurs; alternatively, one may say that for a given impurity concentration, the Mott transition will occur at some critical value of the magnetic field, which we calculate later. For the moment, we return to the work of Yafet, Keyes and Adams since, although they do not consider the role of overlap between neighbouring atoms, their calculation has certain features in common with our own.

They carry out a variational calculation of the ground-state energy, taking as their normalized trial wave-function

$$\phi_{YKA} = (2^{3/2}a^2b\pi^{3/2})^{-\frac{1}{2}} \exp\left(-\frac{x^2+y^2}{4a^2} - \frac{z^2}{4b^2}\right) \qquad (2.2)$$

and writing the Hamiltonian for a hydrogen atom in a uniform magnetic field as

$$H_{YKA} = \frac{p^2}{2m} + \frac{1}{2}\hbar\omega_c L_z + \frac{1}{8}m\omega_c^2 (x^2+y^2) - \frac{e^2}{r} \qquad (2.3)$$

where p is the momentum of the electron, L_z is the dimensionless operator for the component of orbital angular momentum in the field direction (along the z-axis), and ω_c is the cyclotron frequency. They obtain, for a trial value of the ground state energy,

$$E_{YKA} = \frac{1}{2a^2}\left(1 + \frac{d^2}{2}\right) + \frac{\gamma^2 a^2}{2} - \frac{d\sqrt{2}}{a\sqrt{\pi}\sqrt{(1-d^2)}} \ln\left[\frac{1+\sqrt{(1-d^2)}}{1-\sqrt{(1-d^2)}}\right] \tag{2.4}$$

in which $d = \frac{a}{b}$ (2.5)

On minimizing E_{YKA} with respect to a and d the following two equations are obtained:

$$-\frac{1}{a^3}\left(1 + \frac{d^2}{2}\right) + \gamma^2 a + \frac{d\sqrt{2}}{a^2\sqrt{\pi}\sqrt{(1-d^2)}} \ln\left(\frac{1+\sqrt{(1-d^2)}}{1-\sqrt{(1-d^2)}}\right) = 0 \tag{2.6}$$

$$\frac{d}{2a^2} + \frac{\sqrt{2}}{a\sqrt{\pi}}\left\{\frac{2}{1-d^2} - \frac{1}{(1-d^2)^{3/2}} \ln\left[\frac{1+\sqrt{(1-d^2)}}{1-\sqrt{(1-d^2)}}\right]\right\} = 0 \tag{2.7}$$

These two equations are solved numerically for different values of γ and the results are plotted in Fig. 1, which shows how a and b

vary with magnetic field. Fig. 1 also shows how r_o, the spatial extent of the wave function of a free carrier, varies with magnetic field. This is calculated by noting that in a magnetic field, B, a free electron with velocity v will move in a circular orbit, perpendicular to B, whose radius, r, is given by

$$r = \frac{mvc}{eB} \tag{2.8}$$

Hence

$$r^2 = \frac{mvrc}{eB} \tag{2.9}$$

Since, semi-classically, the angular momentum, mvr, is quantized with allowed values $n\hbar$, where n is an integer, the ground state radius is given by

$$r_o = \left(\frac{\hbar c}{eB}\right)^{\frac{1}{2}} \tag{2.10}$$

Fig. 1 justifies the assertion, made earlier, that as the magnetic field increases the atom shrinks in all dimensions.

From (2.4) the ionization energy, E_B, which is the difference between the energies of the lowest bound state and the lowest free state, is readily obtained since, from the definition of γ,

$$E_B = \gamma - E_{YKA} \tag{2.11}$$

where the numerical values of a and b obtained from (2.6) and (2.7) are inserted in E_{YKA}. A graph of E_B as a function of magnetic field is shown in Fig. 2. Yafet et al estimate that their values for E_B are in error by no more than 15%.

They go on to consider the feasibility of an experimental test of their theory. They point out that the magnetic field for which $\gamma = 1$ is given by

$$B_{(\gamma=1)} = 2 \times 10^9 \frac{m^{*2}}{m^2 \epsilon_o^2} \text{ gauss} \qquad (2.12)$$

in which m is the mass of a free electron, m^* is the effective electron mass, ϵ_o is the background dielectric constant of the crystal. For indium antimonide taking $m^* = 10^{-2} m$ and $\epsilon_o = 16$,

$$B_{(\gamma=1)} \simeq 10^3 \text{ gauss},$$

a value readily attained in the laboratory.

Keyes and Sladek (Ref. 7) have measured the conductivity of In Sb as a function of magnetic field, and we shall discuss their results later. They point out, and we emphasize here, that the theory of Yafet, Keyes and Adams is not directly applicable to their results since it does not consider the question of overlap.

2.2 The Work of Fenton and Haering

Fenton and Haering (Ref. 5) have carried out a variational calculation of the binding energy of an impurity electron in a magnetic field; their calculation is essentially similar to that of Yafet, Keyes and Adams, but takes into account the effect of screening by electrons in the conduction band. They argue that, while an increase in the magnetic field increases the binding energy, an increase in the concentration of screening electrons in the conduction band will shift the impurity levels upwards and hence result in a decrease of the binding energy; there will be some critical concentration of conduction electrons such that the lowest state of the impurity will have zero binding energy and for concentrations greater than this, there will be no bound states. Suppose now that we have a doped semiconductor with enough electrons in the conduction band to screen the impurity ions completely. If we now increase the magnetic field from zero a point will be reached at which the concentration of conduction electrons will be only just sufficient to prevent the binding of electrons to the impurities; an infinitesimal increase of the magnetic field beyond this point will introduce bound states. Electrons which become bound will decrease the electron concentration in the conduction band, the screening is reduced and the binding energy increases, introducing yet more bound states. The process is regenerative and the number of electrons in the conduction band will decrease sharply as the magnetic

field is increased.

Fenton and Haering take a trial wave function of the form

$$\phi_{FH} = \left(\pi^{\frac{1}{2}} a b^{\frac{1}{2}}\right)^{-1} \exp\left(-\frac{x^2+y^2}{a^2} - \frac{z^2}{b^2}\right)^{\frac{1}{2}} \tag{2.13}$$

and write the Hamiltonian operator as

$$H_{FH} = \frac{p^2}{2m} + \frac{1}{2}\hbar\omega_c L_z + \frac{1}{8} m\omega_c^2 (x^2+y^2) - \frac{e^2}{r} \exp(-\lambda r) \tag{2.14}$$

in which the Coulomb potential, the last term in (2.14), contains the screening length, $1/\lambda$ (cf. Equation (2.3)).

Hence Fenton and Haering obtain for the trial value of the ground state energy:

$$E_{FH} = \frac{1}{a^2}\left(1 - \frac{\varepsilon}{3}\right) + \gamma^2\frac{a^2}{2} - \frac{(1-\varepsilon)^{\frac{1}{2}}}{a}\left\{\frac{1}{\varepsilon^{\frac{1}{2}}\alpha^{3/2}} \ln\left[\frac{\alpha^{\frac{1}{2}} + \varepsilon^{\frac{1}{2}}}{\alpha^{\frac{1}{2}} - \varepsilon^{\frac{1}{2}}}\right] - \frac{1}{\varepsilon^{\frac{1}{2}}\alpha^{3/2}} \ln\left[\frac{\alpha^{\frac{1}{2}} + \varepsilon^{\frac{1}{2}}\left[(1-\alpha)/(1-\varepsilon)\right]^{\frac{1}{2}}}{\alpha^{\frac{1}{2}} - \varepsilon^{\frac{1}{2}}\left[(1-\alpha)/(1-\varepsilon)\right]^{\frac{1}{2}}}\right] - \frac{2(1-\alpha)^{\frac{1}{2}}}{\alpha(\alpha-\varepsilon)}\left[(1-\alpha)^{\frac{1}{2}} - (1-\varepsilon)^{\frac{1}{2}}\right]\right\} \tag{2.15}$$

where $\alpha = 1-\lambda^2 a^2$ (2.16)

and $\varepsilon = 1 - \frac{a^2}{b^2}$, the eccentricity. (2.17)

If we allow the screening length to become infinite (i.e., we neglect screening) by setting $\lambda = 0$, $\alpha = 1$ in (2.15) we retrieve the expression for the energy obtained by Yafet, Keyes and Adams though with slightly different numerical coefficients owing to the difference between the two trial wave functions.

The numerical results obtained by Fenton and Haering (see Fig. 3) suggest that in indium antimonide at 3.5°K with an impurity concentration of 5.7×10^{15} cm^{-3} the reduction in the number of conduction electrons due to the regenerative process described above takes place at a field of about 20 kilogauss.

2.3 The Work of Durkan and March

Durkan and March (Ref. 8) have carried out a more detailed investigation of the effect of a magnetic field on impurity states in n-type In Sb, considering in addition to screening by conduction electrons the role played by the first excited state of the impurity. To deal with screening they invoke the theory developed by Hebborn and March (Ref. 9) for the screening of a point ion in a metal in the presence of a weak magnetic field and the extension of this theory to fields of arbitrary strength by Durkan, Hebborn and March (Ref. 10). They assume that the electron wave functions are plane waves, modified by the magnetic field, B in the z-direction and consider the electrons to move in a weak potential field, $V(\underset{\sim}{r})$, due to the charged impurity center plus the charge displaced in the conduction band by the charged center. They obtain the following expression for the screened potential to first order, written in terms of the Fourier transform, $\tilde{V}(q)$, where $\underset{\sim}{q}$ is the wave-vector:

$$\tilde{V}(q) = 4\pi e \left\{ (2\pi)^{3/2} \left(\varepsilon_o q^2 + 4\pi e^2 n_o \beta \int_0^1 dy \exp \left\{ - \frac{q_z^2 \hbar^2}{8m^*} \beta(1-y^2) \right\} \right. \right.$$

$$\left. \left. \times \exp \left[- \frac{(q_x^2+q_y^2)\hbar^2}{4m^* \mu_o^* B} \left\{ \coth(\mu_o^* B\beta) - \frac{\cosh(\mu_o^* B\beta y)}{\sinh(\mu_o^* B\beta)} \right\} \right] \right) \right\}^{-1} \qquad (2.18)$$

in which ε_o is the background dielectric constant

n_o is the electron number density

$\beta = \frac{1}{k_B T}$ (k_B is Boltzmann's constant)

$\mu_o^* = \frac{e\hbar}{2m^* c}$, the effective Bohr magneton.

2.3.1 Ground-state

Durkan and March use this screened potential to carry out a variational calculation of the ground-state energy of an impurity, taking a trial wave-function of the same form as that used by Yafet, Keyes and Adams, viz.

$$\phi_o = A \exp\left[- \frac{x^2+y^2}{a^2} - \frac{z^2}{b^2} \right] \tag{2.19}$$

The variational energy is given by

$$E_o = \langle \phi_o | H_o | \phi_o \rangle - e \langle \phi_o | V | \phi_o \rangle$$

$$= \langle H_o \rangle - e \langle V \rangle \tag{2.20}$$

where H_o is the Hamiltonian for an electron in a homogeneous magnetic field, given by

$$H_o = \frac{1}{2m^*} \left(\underset{\sim}{p} + \frac{e}{c} \underset{\sim}{A} \right)^2 \tag{2.21}$$

with $\underset{\sim}{A} = (-\tfrac{1}{2}By, \tfrac{1}{2}Bx, 0)$ (2.22)

Using (2.19) they find

$$\langle V\rangle = \frac{4\pi e}{(2\pi)^3}\iiint\left\{\exp\frac{(q_z^2 b^2)}{8}\ \exp\frac{(-q_\perp^2 a^2)}{8}\ q_\perp dq_\perp dq_z d\phi\right.$$

$$\times\left(\varepsilon_o q^2+4\pi e^2 n_o\beta\int_0^1 dy\ \exp\left\{\frac{-q_z^2\hbar^2 B}{8m^*}(1-y^2)\right\}\right.$$

$$\left.\left.\times\exp\left[\frac{-q_\perp^2\hbar^2}{4m^*\mu_o^* B}\left\{\coth(\mu_o^* B\beta)-\frac{\cosh(\mu_o^* B\beta y)}{\sinh(\mu_o^* B\beta)}\right\}\right]\right)^{-1}\right\} \qquad (2.23)$$

and

$$\langle H_o\rangle = \frac{e^2B^2a^2}{16m^*c^2}+\frac{\hbar^2}{2m^*}\left(\frac{2}{a^2}+\frac{1}{b^2}\right) \qquad (2.24)$$

For the binding energy they thus obtain:

$$E_b = \frac{\hbar^2}{m^*a^2}\left(1+\frac{a^2}{2b^2}\right)+\frac{e^2B^2}{16m^*c^2}\cdot\frac{4\hbar c}{eB}-\frac{\hbar eB}{2m^*c}$$

$$-\frac{4e^2}{2\pi}\left(\frac{8}{a^2}\right)^{\frac{1}{2}}\int_0^\infty dq_z\int_0^\infty\left\{\exp\left\{-q_z^2\left(\frac{b}{a}\right)^2\right\}\ \exp(-q_\perp^2)q_\perp dq_\perp\right.$$

$$\times\left(q^2+\frac{\pi n_o e^2\beta a^2}{2}\int_0^1 dy\ \exp\left\{\frac{-q_z^2\hbar^2\beta}{m^*a^2}(1-y^2)\right\}\right.$$

$$\left.\left.\times\exp\left[\frac{-q^2\,2\hbar^2}{m^*\mu_o^* Ba^2}\left\{\coth(\mu_o^* B\beta)-\frac{\cosh(\mu_o^* B\beta y)}{\sinh(\mu_o^* B\beta)}\right\}\right]\right)^{-1}\right\} \qquad (2.25)$$

E_b is a function not only of the variational parameters a and b, but also of B, T and n_o. Durkan and March minimized the energy with respect to the parameter, d, defined by

$$d = \frac{b}{a} \tag{2.26}$$

and some of their results are shown in Fig. 4, in which the ionization energy is shown as a function of n_o. The curves 1 to 4 were constructed for four samples of InSb with different donor and acceptor concentrations, N_d and N_a (shown in Table 1 below), using the relation:

$$\frac{Na + N_o}{N_d - N_a - n_o} = n_o^{-1} N \exp\left(-\frac{Eionization}{k_B T}\right) \tag{2.27}$$

where

$$N = (2\pi m^* k_B T)^{\frac{1}{2}} \frac{eB}{h^2 c} \tag{2.28}$$

The values of B and T used were

B = 5000 gauss

T = 3°K.

Table 1

Sample	$N_d \times 10^{-13}$	$N_a \times 10^{-13}$
1	100	98
2	43	38
3	24	21
4	45	38

Curve 5 shows the effect of screening; where it crosses curves 1 to 4 the new ionization energy is obtained; for the samples considered the reduction of ionization energy by screening is only a few percent. The importance of screening is more evident when the first excited state is considered. The experimentally determined activation energy is shown as a function of B for the same four samples in Fig. 5.

2.3.2 First Excited State

In considering the first excited state Durkan and March assume that the excited states have broadened into a band forming a quasi-continuum with the conduction band and derive an approximate expression for the activation energy by estimating the energy difference between the first excited state and the ground state. They take as their trial wave function

$$\phi_1 = \frac{\exp(-i\phi)}{(2\pi)^{\frac{1}{2}}} \quad \frac{\exp(-z^2/b^2)}{b^{\frac{1}{2}}} \left(\frac{2}{\pi}\right)^{\frac{1}{4}} \quad \frac{4r \exp(-r^2/a^2)}{2^{\frac{1}{2}} a^2} \tag{2.29}$$

The mean values of H_o and V are then found to be

$$\langle H_o \rangle = \frac{\hbar eB}{8m^*c} \quad \frac{1}{d} + \frac{\hbar eB}{2m^*c} \tag{2.30}$$

and

$$\langle V \rangle = \frac{e^2}{\varepsilon_o \pi} \left(\frac{2eB}{\hbar c} \right)^{\frac{1}{2}} \int_0^\infty dq_z \exp(-q^2{}_z d^2) \int_0^\infty \left\{ 2q_\perp dq_\perp (1-q^2{}_\perp) \exp(-q^2{}_\perp) \right.$$

$$\times \left(q^2 + \frac{2\pi n_o \beta e \hbar c}{\varepsilon_o B} \int_0^1 dy \exp \left\{ -q^2{}_z (1-y^2) \frac{\mu_o{}^* B\beta}{2} \right\} \right.$$

$$\left. \left. \times \exp \left[-q^2_\perp \left\{ \coth(\mu_o{}^* B\beta) - \frac{\cosh(\mu_o{}^* B\beta y)}{\sinh(\mu_o{}^* B\beta)} \right\} \right] \right)^{-1} \right\} \qquad (2.31)$$

The energy is calculated as before, using

$$E = \langle H_o \rangle - e \langle V \rangle \qquad (2.32)$$

and minimized with respect to the parameter d defined in (2.26). The resulting ionization energy, for B = 5000 gauss and T = 3^oK, is shown in curve 6 of Fig. 4; the effect of screening on the ionization energy is much greater for the first excited state than for the ground state.

Durkan and March go on to emphasize the importance of the part played by the first excited state when the overlap between neighbouring wave functions is considered; they quote, from the calculation of Wallis and Bowlden (Ref. 11), typical values of the parameter d (=b/a) for the ground state and the first excited state in various magnetic fields, as shown in the following table:

Table 2

B (x 10^3 gauss)	d in Coulomb field	
	ground state	first excited state
5	1.2	1.7
	1.3	1.8
9	1.4	1.9

The overlap is seen to be greater for the first excited state than for the ground state, and the role of the excited states in a consideration of the Mott transition will clearly be significant.

SECTION 3. The Dielectric Approach to Impurity Conduction.

3.1 The Criterion for Impurity Conduction.

Frood (Ref. 12) has used an entirely different approach to impurity conduction in semiconductors, using the theory of dielectrics and including the effect of excited states. Considering the same model of hydrogen-like impurities in a background of dielectric constant ε_o, he invokes the Clausius - Mossotti formula for the dielectric constant, ε_s, of the whole system; for the ground-state, at $T = 0^oK$, this is:

$$\frac{\varepsilon_s - \varepsilon_o}{\varepsilon_s + 2\varepsilon_o} = \frac{4\pi}{3\varepsilon_o} N\alpha_1 \qquad (3.1)$$

where N is the number density of donor impurities and α_1 is the ground-state polarizability. The idea is then that the system behaves as a metallic conductor when ε_s becomes very large. This gives, from (3.1), the condition

$$\frac{4\pi}{3\varepsilon_o} N\alpha_1 = 1 \qquad (3.2)$$

when conduction takes place. For $T > 0^oK$ the contribution to the permittivity of electrons in excited states must also be taken into account and this is done by adding together the polarizations of all

levels of principal quantum number n = 1, 2, 3, ... n' to give the total polarization. Frood points out that the total number, n', of discrete levels cannot be taken as infinite (as for an isolated atom) since this would result in an infinite permittivity and one could speak only of the metallic properties of the medium; the excited levels for which $n > n'$ are considered to be catastrophic, in the sense of the Clausius - Mossotti formula, and are to be associated with metallic conduction. Thus n' is defined as the highest possible non-catastrophic principal quantum number compatible with a given temperature and donor concentration and the permittivity of the donors and background is thus maintained finite and positive; essentially one assumes that all catastrophic excited states merge with the continuum.

The importance of the excited states is emphasized by Frood in the following argument. The catastrophe in level n occurs when

$$\frac{4\pi}{3\varepsilon_o} A_n \alpha_n = 1 \tag{3.3}$$

where α_n, the polarizability of this level is given by

$$\alpha_n \simeq n^6 a^3_H \tag{3.4}$$

a_H being the ground-state Bohr radius, and A_n is the population density of the n-th level. A_n is given by

$$A_n = A(T) \frac{n^2 \exp(-E_n/k_BT)}{\sum_{n=1}^{n'} n^2 \exp(-E_n/k_BT)} \tag{3.5}$$

in which A(T) is the number density of un-ionized donors and E_n, the energy of the level measured from the ground-state, is given by

$$E_n = I_o \left(1 - \frac{1}{n^2}\right) \tag{3.6}$$

where I_o is the ionization energy of the ground level. The factor n which occurs in the numerator and denominator of (3.5) arises from the degeneracy of the n-th level. From (3.4), (3.5), and (3.6) we find that

$$\frac{A_n \alpha_n}{A_1 \alpha_1} \simeq n^8 \exp\left[-\frac{T_o}{T}\left(1 - \frac{1}{n^2}\right)\right] \tag{3.7}$$

where $T_o = I_o/k_B$ (3.8)

Hence if $T > \frac{T_o(1-1/n^2)}{8 \ln n}$ (3.9)

the ratio $\frac{A_n \alpha_n}{A_1 \alpha_1}$ is greater than unity and the dielectric catastrophe will occur first in the excited level. With n = 2, for example, the first excited state becomes catastrophic before the ground state if $T > 16^oK$. Similarly, the level for which n = 5 becomes catastrophic

before the ground state if $T > 6.8^{o}K$. Clearly the excited levels are important in deciding when conduction occurs and Frood's treatment of this question and his determination of what value to give to n', the highest level to be included, are given in detail in the next section.

3.2 The Dielectric Constant of the Donors and Crystal.

To calculate the dielectric constant of the donor atoms plus the background crystal, Frood notes that when an electric field is applied the energy of the n-th level is altered and, considering only the linear and quadratic effects, splits into a number of pairs of levels given by

$$E^{(\pm)}_{n,\lambda}(m) = E_n \pm \mu_{n,\lambda} f_{n,\lambda}(m) - \frac{1}{2}\alpha_{n,\lambda} f^2_{n,\lambda}(m) \qquad (3.10)$$

where n and m are the principal and magnetic quantum numbers respectively and λ is a positive integer ($1 \leq \lambda \leq n$) designating the pair of levels considered. $f_{n,\lambda}(m)$ is the local field acting on the electron in the state (n,λ,m) and $\alpha_{n,\lambda}$ is the corresponding polarizability. Frood then quotes the following relations from Condon and Shortley (Ref. 13):

$$\mu_{n,\lambda} = \frac{3}{2} a_H e n(n-\lambda) \qquad (3.11)$$

$$\alpha_{n,\lambda}(m) = \frac{1}{8} a_H^3 n^4 (14n^2 + 6n\lambda - 3\lambda^2 - 9m^2 + 19) \qquad (3.12)$$

where m assumes a total of λ values given by

$$m = (\lambda-1), (\lambda-3), \ldots\ldots -(\lambda-3), -(\lambda-1) \qquad (3.13)$$

We see from (3.11) and (3.13) that $\lambda = n$ leads to n non-polar states while the remaining values of λ lead to n^2-n polar states of the original level. Frood then assumes that for weak local fields such that

$$\mu_{n,\lambda} f_{n,\lambda} << k_B T \tag{3.14}$$

the field has no effect on the partition function of the donor atom (the denominator of (3.5)). The number density of electrons in upper and lower dipolar states is then, by (3.10),

$$A_{n,\lambda}^{(\pm)}(m) = A_n \left(\frac{\lambda}{n^2}\right) \exp\left(\frac{\mp \mu_{n,\lambda} f_{n,\lambda}(m)}{k_B T}\right) \tag{3.15}$$

and for the non-polar states ($\lambda = n$)

$$A_{n,n} = \frac{n}{n^2} A_n \tag{3.16}$$

where A_n is given by (3.5).

The polarizability given by (3.12) is averaged over the allowed values of m and the dielectric constant is then calculated on the basis of the Onsager formula (Ref. 14), taking account of the dielectric constant of the background crystal, as follows.

The number density of particles in the state (n,λ) is, from (3.15) for weak local fields,

$$A_{n,\lambda} = A_{n,\lambda}^{(\pm)} + A_{n,\lambda}^{(-)} = \frac{2\lambda}{n^2} A_n \tag{3.17}$$

and so, by the Onsager formula, the polarization due to polar donors in this state is

$$\underset{\sim}{P}_{n,\lambda} = \frac{(2\lambda/n^2)\, A_n}{1 - \alpha_{n,\lambda}\, g_{n,\lambda}} \left\{ \alpha_{n,\lambda} + \frac{\mu^2_{n,\lambda}}{(1 - \alpha_{n,\lambda} g_{n,\lambda}) k_B T} \right\} \underset{\sim}{F}_c \qquad (3.18)$$

where $\underset{\sim}{F}_c$ is the cavity field given by

$$\underset{\sim}{F}_c = \frac{3\varepsilon_s}{2\varepsilon_s + \varepsilon_o} \underset{\sim}{F} \qquad (3.19)$$

and $\underset{\sim}{F}$ is the macroscopic field. $g_{n,\lambda}$ is the reaction field factor given by

$$g_{n,\lambda} = \frac{2(\varepsilon_s - \varepsilon_o)}{\varepsilon_o(2\varepsilon_s + \varepsilon_o)} \cdot \frac{1}{r^3_{n,\lambda}} \qquad (3.20)$$

where $r_{n,\lambda}$ is obtained from the atomic volume of donors in the state (n,λ) using (3.17):

$$\frac{1}{r^3_{n,\lambda}} = \frac{4\pi}{3} A_{n,\lambda} = \frac{8\pi\lambda}{3n^2} A_n \qquad (3.21)$$

Similarly the polarization due to non-polar states (n,n) is

$$\underset{\sim}{P}_{n,n} = \frac{(n/n^2)A_n}{1 - \alpha_{n,n} g_{n,n}} \alpha_{n,n} \underset{\sim}{F}_c \qquad (3.22)$$

On adding (3.18) and (3.22), summing over all bound states and add-

ing the polarization of the background crystal we get

$$\frac{(\varepsilon_s-\varepsilon_o)(2\varepsilon_s+\varepsilon_o)}{12\pi\,\varepsilon_s} = \sum_{n=1}^{n'} \frac{A_n}{1-\alpha_n g_n} \left\{ \alpha_n + \frac{\mu_n^2}{(1-\alpha_n g_n) k_B T} \right\} \tag{3.23}$$

where

$$\alpha_n = \frac{3}{8} a_H^3 \, n^4 (5n^2+7) \tag{3.24}$$

and

$$\mu_n^2 = \frac{3}{8} a_H^2 \, e^2 n^2 (n^2-1) \tag{3.25}$$

are the average polarizability and squared dipole moment for the n-th level and

$$g_n = \frac{4\pi}{3\varepsilon_o} \left\{ \frac{2(\varepsilon_s-\varepsilon_o)}{2\varepsilon_s+\varepsilon_o} \right\} A_n \tag{3.26}$$

is the average reaction field factor for this level.

At first sight it seems that if we set $T = 0^oK$ in (3.23) then ε_s must become infinite, suggesting that the system will always behave like a metallic conductor at absolute zero! We note, however, that when $T = 0^oK$ there will be no excited states; hence the population density, A_n, will be zero unless $n = 1$ and, moreover, when $n = 1$ we see from (3.25) that $\mu_n = 0$. In fact, the dielectric catastrophe always occurs through the polarizability, not through the intrinsic dipole moment, and this is true even at absolute zero.

Frood now argues that if (3.23) is to represent a finite dielectric constant n' must be so chosen that the factors $1-\alpha_n g_n$ are positive for all $1 \leq n \leq n'$, since the levels having $n > n'$ for which $1-\alpha_n g_n \leq 0$ lead to infinite or negative polarizations associated with conduction.

Frood goes on to show that infinite values of ε_s in (3.23) are catastrophic in the same sense as implied by the Clausius-Mossotti formula (3.1): supposing that as $n \to n'$, $1-\alpha_n g_n \to 0$ then only the n'-th term in (3.23) makes a significant contribution; since the catastrophe occurs through the polarizability we may omit the dipolar term in μ_n^2 from (3.23) to get

$$\frac{(\varepsilon_s-\varepsilon_o)(2\varepsilon_s+\varepsilon_o)}{12\pi\varepsilon_s} \simeq \frac{A_{n'}\alpha_{n'}}{1-\alpha_{n'}g_{n'}} \tag{3.27}$$

and, from (3.26),

$$g_{n'}\alpha_{n'} = \frac{8\pi}{3\varepsilon_o} \frac{(\varepsilon_s-\varepsilon_o)}{(2\varepsilon_s+\varepsilon_o)} A_{n'}\alpha_{n'} \tag{3.28}$$

Hence

$$\frac{(\varepsilon_s-\varepsilon_o)(2\varepsilon_s+\varepsilon_o)}{12\pi\varepsilon_s} \simeq \frac{A_{n'}\alpha_{n'}}{1 - \frac{8\pi}{3\varepsilon_o} \frac{(\varepsilon_s-\varepsilon_o)}{(2\varepsilon_s+\varepsilon_o)} A_{n'}\alpha_{n'}} \tag{3.29}$$

This is an equation for $A_{n'}\alpha_{n'}(=x)$ of the form

$$A = \frac{x}{1-Bx}$$

$$x = \frac{A}{1+AB}$$

$$\text{i.e.} \quad A_n'\alpha_n' \simeq \frac{(\varepsilon_s-\varepsilon_o)(2\varepsilon_s+\varepsilon_o)/12\pi\varepsilon_s}{1 + \frac{(\varepsilon_s-\varepsilon_o)(2\varepsilon_s+\varepsilon_o)}{12\pi\varepsilon_s} \frac{8\pi}{3\varepsilon_o} \frac{(\varepsilon_s-\varepsilon_o)}{(2\varepsilon_s+\varepsilon_o)}}$$

$$= \frac{(\varepsilon_s-\varepsilon_o)(2\varepsilon_s+\varepsilon_o)}{12\pi\varepsilon_s + \frac{8\pi}{3\varepsilon_o}(\varepsilon_s-\varepsilon_o)^2}$$

On expanding and factorizing this leads to

$$\frac{4\pi}{3\varepsilon_o} A_n'\alpha_n' = \frac{\varepsilon_s-\varepsilon_o}{\varepsilon_s+2\varepsilon_o} \tag{3.30}$$

which is the same as (3.1) if we replace A_n' by N and α_n', by α'.

In our own work, described in the next section, we adopt the dielectric approach of Frood, summarized above.

SECTION 4. Calculation of the Magnetic Field required to Reverse the Mott Transition.

4.1 The Basic Model.

We have already noted (see page 7, above) that the application of a strong magnetic field to a hydrogen atom results in a shrinkage of the charge distribution in all its dimensions; if the concentration of atoms is great enough (i.e. the spacing is small enough) for the Mott transition to have taken place, so that the system is conducting, it may then be possible for the magnetic field to decrease the overlap between neighbouring atoms to such an extent that the Mott transition is reversed and the system becomes non-conducting. In this section we calculate the magnetic field required to bring about this transition from the conducting to the non-conducting state.

We adopt the dielectric approach of Frood, outlined in Section 3 above, taking for our model hydrogen-like impurities in a crystal providing a background of dielectric constant, ε_o; we assume that $T = 0^oK$, so that there are no electrons in the conduction band (i.e. we do not consider the effects of screening by conduction electrons) and the impurities are all in the ground state (i.e. they have no intrinsic electric dipole moment). We then carry out a variational calculation of the average polarizability, $\bar{\alpha}$, of an impurity in a magnetic field, B. The permittivity, ε_s, of the crystal and impurities together is then

given by the Clausius-Mossotti formula,

$$\frac{\varepsilon_s - \varepsilon_o}{\varepsilon_s + 2\varepsilon_o} = \frac{4\pi}{3\varepsilon_o} N\bar{\alpha} \tag{4.1}$$

where N is the impurity concentration. We assume that conduction occurs when ε_s becomes very large, giving the criterion, from (4.1)

$$\frac{4\pi}{3\varepsilon_o} N\bar{\alpha} = 1 \tag{4.2}$$

It turns out that α decreases as B increases, so (4.2) determines the critical value of B required to make the system non-conducting. The immediate problem, then, is to determine $\bar{\alpha}$ as a function of B.

4.2 Calculation of the Polarizability.

We consider the impurity in the presence of a uniform magnetic field, $\underset{\sim}{B}$, and a small perturbing uniform electric field, $\underset{\sim}{F}$. Our procedure is then as follows. We choose a normalized trial wave function, ϕ, containing certain parameters and calculate the energy, E, given by

$$E = \int \phi^* H \phi \, d\tau \tag{4.3}$$

where H is the Hamiltonian operator and $d\tau$ is the volume element. The resulting expression for E is minimized with respect to each of the parameters contained in ϕ to give E_{min}. E_{min} will contain

a term, E_F, proportional to F^2 and the polarizability, α, is then found by noting that

$$E_F = -\tfrac{1}{2}\alpha F^2 \tag{4.4}$$

In general, $\underset{\sim}{B}$ and $\underset{\sim}{F}$ will not be in the same direction so we consider separately the cases in which $\underset{\sim}{F}$ is parallel to and perpendicular to $\underset{\sim}{B}$, obtaining polarizabilities α_{11} and $\alpha_{\perp}$. The average polarizability, $\bar{\alpha}$, is then chosen as

$$\bar{\alpha} = (\alpha_{11} + 2\alpha_{\perp})/3 \tag{4.5}$$

The propriety of such a definition of $\bar{\alpha}$ is discussed later.

4.3 Calculation of α_{11}.

We use cylindrical polar co-ordinates (r, θ, z) and choose the z-axis to be in the direction of the magnetic field, $\underset{\sim}{B}$, which we specify by means of a magnetic vector potential, $\underset{\sim}{A}$, whose components are given by

$$\underset{\sim}{A} = (0, \tfrac{1}{2}Br, 0) \tag{4.6}$$

This choice of A gives a uniform field of magnitude B in the z-direction as required and also satisfies

$$\underset{\sim}{\nabla} \cdot \underset{\sim}{A} = 0$$

In the present case the uniform electric field, $\underset{\sim}{F}$,

is also in the z-direction and its components are therefore given by

$$\underset{\sim}{F} = (0,\ 0,\ F) \tag{4.7}$$

The Hamiltonian operator for our system is then given by

$$H = \frac{1}{2m}\left(\frac{\hbar}{i}\underset{\sim}{\nabla} + \frac{e}{c}\underset{\sim}{A}\right)^2 - \frac{e^2}{(r^2 + z^2)^{\frac{1}{2}}} + Fez \tag{4.8}$$

in which m is the effective mass of the electron, e is the magnitude of the effective electronic charge, given by

$$e = (\text{actual electronic charge})/\sqrt{\varepsilon_o}$$

where ε_o is the dielectric constant of the background valence crystal.

We now choose our trial function, ϕ, to be

$$\phi = C_{11} \exp\left[-\left(\frac{r^2}{a^2} + \frac{z^2}{b^2}\right)^{\frac{1}{2}}\right] (1 + \beta z) \tag{4.9}$$

in which a, b and β are the parameters to be varied in minimizing E and C_{11} is a normalizing constant whose value is determined by satisfying the equation

$$\int \phi^* \phi \, d\tau = 1$$

This gives

$$C_{11} = 1/\left[\pi b(1 + \beta^2 b^2)\right]^{\frac{1}{2}} a \tag{4.10}$$

The trial function given by (4.9) differs from that used by Fenton and Haering (Ref. 5) only by the additional factor $(1 + \beta z)$ which is introduced here because we have an electric field in the z-direction. Roughly speaking, the parameter β accounts for distortion in the z-direction due to the electric field while the parameters a and b (or, more accurately, their ratio) describe the departure from sphericity due to the magnetic field. Clearly, if we set $a = b$, $\beta = 0$ we recover the wave function for the ground state of the hydrogen atom.

Calculation of the energy E from (4.3), using equations (4.6) to (4.10), gives:

$$E_{11} = \frac{1}{1 + \beta^2 b^2} \left\{ \frac{\hbar^2}{m} \left[\frac{1}{3a^2} + \frac{1}{6b^2} + \frac{\beta^2 b^2}{5a^2} + \frac{3\beta^2}{10} \right] \right.$$

$$+ \frac{e^2 B^2}{4mc^2} \left[a^2 + \frac{3\beta^2}{2} a^2 b^2 \right]$$

$$+ \frac{e^2}{2b} \left[\varepsilon^{-\frac{1}{2}} \ln \left(\frac{1 - \varepsilon^{\frac{1}{2}}}{1 + \varepsilon^{\frac{1}{2}}} \right) - \frac{3}{4} \beta^2 a^2 \left(\varepsilon^{-3/2} \ln \left(\frac{1 - \varepsilon^{\frac{1}{2}}}{1 + \varepsilon^{\frac{1}{2}}} \right) + \frac{2}{\varepsilon(1-\varepsilon)} \right) \right]$$

$$\left. + \frac{2Fe\beta a^2}{1 - \varepsilon} \right\} \qquad (4.11)$$

where

$$\varepsilon = 1 - \frac{a^2}{b^2} \qquad (4.12)$$

As a check we note that in the absence of any fields (i.e. if we set B = 0, β = 0 and a → b, ϵ → 0) equation (4.11) reduces to

$$E_{11} = -\frac{e^2}{2a_H}$$

where a_H, the effective Bohr radius, is given by

$$a_H = \frac{\hbar^2}{me^2} \tag{4.13}$$

Moreover, if we set β = 0 equation (4.11) is identical with the expression for E given by Fenton and Haering (equation (12) of Ref. 5) if we neglect screening effects and take into account the units used in Ref. 5.

We now minimize E with respect, firstly, to the parameter β. In doing so we shall assume that the field F, and hence the parameter β, are small. Equation (4.11) may be written

$$E_{11} = (1 + \beta^2 b^2)^{-1} \{X + 2Feb^2\beta + Y\beta^2\} \tag{4.14}$$

where

$$X = \frac{\hbar^2}{m}\left[\frac{1}{3a^2} + \frac{1}{6b^2}\right] + \frac{e^2B^2a^2}{4mc^2} + \frac{e^2}{2b}\epsilon^{-\frac{1}{2}}\ln\left(\frac{1-\epsilon^{\frac{1}{2}}}{1+\epsilon^{\frac{1}{2}}}\right) \tag{4.15}$$

and

$$Y = \frac{\hbar^2}{m}\left[\frac{b^2}{5a^2} + \frac{3}{10}\right] + \frac{e^2B^2}{4mc^2} \cdot \frac{3a^2b^2}{2}$$

$$- \frac{e^2}{2b} \cdot \frac{3a^2}{4}\left(\varepsilon^{-3/2}\ln\left(\frac{1-\varepsilon^{\frac{1}{2}}}{1+\varepsilon^{\frac{1}{2}}}\right) + \frac{2}{\varepsilon(1-\varepsilon)}\right) \qquad (4.16)$$

We now expand (4.14) in powers of β to get

$$E_{11} = X + 2Feb^2\beta + (Y - b^2X)\beta^2 + \text{higher terms} \qquad (4.17)$$

Setting $\frac{\partial E}{\partial \beta} = 0$ we get, neglecting β^2 and higher terms,

$$\beta = - \frac{Feb^2}{Y - b^2X} \qquad (4.18)$$

Substituting this value of β in (4.17) and neglecting powers of F higher than the second we find, using (4.4)

$$\alpha_{11} = \frac{2e^2b^4}{Y - b^2X} \qquad (4.19)$$

where X and Y are defined in (4.15) and (4.16). Of course, we do not yet know what values of a and b should be substituted in (4.19) to give α_{11}, since we have not yet minimized E with respect to these parameters, but even before doing so we may check the validity of (4.19) by putting $B = 0$, $a \to a_H$, $b \to a_H$, $\varepsilon \to 0$ in the expressions

for X and Y. (4.19) then yields the known result

$$\alpha_{11} = 4a_H^3 .$$

Instead of minimizing E with respect to a and b, we shall now work in terms of a and ε, where ε is defined in (4.12). Our expression for E becomes

$$E_{11} = \frac{1}{1 + \frac{\beta^2 a^2}{1-\varepsilon}} \left\{ \frac{\hbar^2}{m} \left[\frac{1}{3a^2} + \frac{1-\varepsilon}{6a^2} + \frac{\beta^2}{5(1-\varepsilon)} + \frac{3\beta^2}{10} \right] \right.$$

$$+ \frac{e^2 B^2}{4mc^2} \left[a^2 + \frac{3\beta^2}{2} \frac{a^4}{1-\varepsilon} \right]$$

$$+ \frac{e^2}{2a} (1-\varepsilon)^{\frac{1}{2}} \left[\varepsilon^{-\frac{1}{2}} \ln \left(\frac{1-\varepsilon^{\frac{1}{2}}}{1+\varepsilon^{\frac{1}{2}}} \right) - \frac{3\beta^2 a^2}{4} \left(\varepsilon^{-3/2} \ln \left(\frac{1-\varepsilon^{\frac{1}{2}}}{1+\varepsilon^{\frac{1}{2}}} \right) \right. \right.$$

$$\left. \left. \left. + \frac{2}{\varepsilon(1-\varepsilon)} \right) \right] + \left. \frac{2Fe\beta a^2}{1-\varepsilon} \right\} \qquad (4.20)$$

Minimizing with respect to a and ε we get, if β is again assumed to be small,

$$\frac{\hbar^2}{2m} \left(1-\frac{\varepsilon}{3}\right) \left(-\frac{2}{a^3}\right) + \frac{e^2 B^2}{2mc^2} a - \frac{e^2}{2a^2} (1-\varepsilon)^{\frac{1}{2}} \varepsilon^{-\frac{1}{2}} \ln \left(\frac{1-\varepsilon^{\frac{1}{2}}}{1+\varepsilon^{\frac{1}{2}}} \right) = 0 \qquad (4.21)$$

and

$$\frac{\hbar^2}{2m} \cdot \frac{1}{3a^2} + \frac{e^2}{4a} \varepsilon^{-3/2}(1-\varepsilon)^{-\frac{1}{2}} \ln\left(\frac{1-\varepsilon^{\frac{1}{2}}}{1+\varepsilon^{\frac{1}{2}}}\right) + \frac{e^2}{2a} \cdot \frac{1}{\varepsilon(1-\varepsilon)^{\frac{1}{2}}} = 0 \qquad (4.22)$$

Summarizing our results then, α_{11} is given by equation (4.19) in which we must substitute the values of a, b and ε given by (4.12), (4.21) and (4.22).

4.4 Calculation of $\alpha_{\perp}$

We proceed along the same lines, but since $\underset{\sim}{F}$ is now perpendicular to $\underset{\sim}{B}$ we choose $\underset{\sim}{F}$ to be in the x-direction with $\underset{\sim}{B}$ in the z-direction as before. The components of $\underset{\sim}{F}$ are therefore given by

$$\underset{\sim}{F} = (F, 0, 0) \qquad (4.23)$$

while $\underset{\sim}{B}$ and the vector potential $\underset{\sim}{A}$ are unchanged.
The Hamiltonian is now given by

$$H = \frac{1}{2m}\left(\frac{\hbar}{i} \underset{\sim}{\nabla} + \frac{e}{c} \underset{\sim}{A}\right)^2 - \frac{e^2}{(r^2 + z^2)^{\frac{1}{2}}} + Fer \cos\theta \qquad (4.24)$$

and we choose a trial wave function given by

$$\phi = C_{\perp} \exp\left[- \left(\frac{r^2}{a^2} + \frac{z^2}{b^2}\right)^{\frac{1}{2}} \right] (1 + \beta r \cos\theta) \qquad (4.25)$$

where the normalizing constant $C_\perp$ is

$$C_\perp = 1/\left[\pi b(1 + \beta^2 a^2)\right]^{\frac{1}{2}} a \tag{4.26}$$

The expression for E, calculated from (4.3) and (4.24) to (4.26) is

$$E_\perp = \frac{1}{1+\beta^2 a^2} \left\{ \frac{\hbar^2}{2m} \left[\frac{2}{3} \cdot \frac{1}{a^2} + \frac{1}{3} \cdot \frac{1}{b^2} \quad \frac{4}{5} \beta^2 + \frac{1}{5} \beta^2 \quad \frac{a^2}{b^2} \right] \right.$$

$$+ \frac{e^2 B^2}{4mc^2} a^2 (1 + 3a^2\beta^2)$$

$$+ \frac{e^2}{2b} \left[\varepsilon^{-\frac{1}{2}} \ln \left(\frac{1-\varepsilon^{\frac{1}{2}}}{1+\varepsilon^{\frac{1}{2}}} \right) + \frac{3}{8} \beta^2 a^2 \left(\varepsilon^{-\frac{1}{2}} \ln \left(\frac{1-\varepsilon^{\frac{1}{2}}}{1+\varepsilon^{\frac{1}{2}}} \right) + \varepsilon^{-3/2} \ln \left(\frac{1-\varepsilon^{\frac{1}{2}}}{1+\varepsilon^{\frac{1}{2}}} \right) \right.\right.$$

$$\left.\left. + \frac{2}{\varepsilon} \right) + 2Fe\beta a^2 \right\} \tag{4.27}$$

This is of the form

$$E_\perp = (1 + \beta^2 a^2)^{-1} \quad (X + 2Fea^2\beta + Z\beta^2) \tag{4.28}$$

where X is given by equation (4.15) and

$$Z = \frac{\hbar^2}{2m} \left[\frac{4}{5} + \frac{1}{5} \cdot \frac{a^2}{b^2} \right] + \frac{e^2 B^2}{4mc^2} \cdot 3a^4$$

$$+ \frac{e^2}{2b} \cdot \frac{3}{8} a^2 \left\{ \varepsilon^{-\frac{1}{2}} \ln \left(\frac{1-\varepsilon^{\frac{1}{2}}}{1+\varepsilon^{\frac{1}{2}}} \right) + \varepsilon^{-3/2} \ln \left(\frac{1-\varepsilon^{\frac{1}{2}}}{1+\varepsilon^{\frac{1}{2}}} \right) + \frac{2}{\varepsilon} \right\} \tag{4.29}$$

Again we minimize with respect to β, neglecting β^2 and higher terms, to get

$$\beta = - \frac{Fea^2}{Z - a^2X} \tag{4.30}$$

leading to a value for the polarizability, $\alpha_\perp$, given by

$$\alpha_\perp = \frac{2e^2a^4}{Z - a^2X} \tag{4.31}$$

In terms of a and ε our expression for E becomes

$$E_\perp = \frac{1}{1 + \beta^2a^2} \left\{ \frac{\hbar^2}{2m} \left[\frac{1}{a^2} \left(1 - \frac{\varepsilon}{3}\right) + \beta^2 \left(1 - \frac{\varepsilon}{5}\right) \right] \right.$$

$$+ \frac{e^2B^2}{4mc^2} a^2(1 + 3a^2\beta^2)$$

$$+ \frac{e^2}{2a} \frac{(1-\varepsilon)^{\frac{1}{2}}}{\varepsilon^{\frac{1}{2}}} \left[\ln\left(\frac{1-\varepsilon^{\frac{1}{2}}}{1+\varepsilon^{\frac{1}{2}}}\right) + \frac{3}{8} \beta^2a^2 \left(\left(1 + \frac{1}{\varepsilon}\right) \ln\left(\frac{1-\varepsilon^{\frac{1}{2}}}{1+\varepsilon^{\frac{1}{2}}}\right) \right.\right.$$

$$\left.\left. + \frac{2}{\varepsilon^{\frac{1}{2}}} \right) + 2Fe\beta a^2 \right\} \tag{4.32}$$

In minimizing with respect to a and ε we again assume β to be small. With this assumption $E_\perp$ is identical in value with $E_{||}$, i.e. equations (4.20) and (4.32) are the same for small β. Hence the equations which determine a and ε are the same as in the parallel case, viz. equations (4.21) and (4.22).

4.5 Numerical Calculations.

For convenience we reproduce here the equations, derived above, which were used in the computer calculation of the average polarizability.

The quantities X, Y and Z are defined by

$$X = \frac{\hbar^2}{2m}\left[\frac{2}{3a^2} + \frac{1}{3b^2}\right] + \frac{e^2B^2}{4mc^2}a^2 + \frac{e^2}{2b}\varepsilon^{-\frac{1}{2}}\ln\left(\frac{1-\varepsilon^{\frac{1}{2}}}{1+\varepsilon^{\frac{1}{2}}}\right) \tag{4.15}$$

$$Y = \frac{\hbar^2}{2m}\left[\frac{2}{5}\cdot\frac{b^2}{a^2} + \frac{3}{5}\right] + \frac{e^2B^2}{4mc^2}\cdot\frac{3}{2}a^2b^2 - \frac{e^2}{2b}\cdot\frac{3}{4}a^2\left[\varepsilon^{-3/2}\ln\left(\frac{1-\varepsilon^{\frac{1}{2}}}{1+\varepsilon^{\frac{1}{2}}}\right) + \frac{2}{\varepsilon(1-\varepsilon)}\right] \tag{4.16}$$

$$Z = \frac{\hbar^2}{2m}\left[\frac{1}{5}\cdot\frac{a^2}{b^2} + \frac{4}{5}\right] + \frac{e^2B^2}{4mc^2}\cdot 3a^4 + \frac{e^2}{2b}\cdot\frac{3}{8}a^2\left[(\varepsilon^{-\frac{1}{2}} + \varepsilon^{-3/2})\ln\left(\frac{1-\varepsilon^{\frac{1}{2}}}{1+\varepsilon^{\frac{1}{2}}}\right) + \frac{2}{\varepsilon}\right] \tag{4.29}$$

The parameters a, b and ε are related by

$$\varepsilon = 1 - \frac{a^2}{b^2} \cdot \tag{4.12}$$

a and ε are the solution of the two equations

$$\frac{\hbar^2}{2m}\left(1-\frac{\varepsilon}{3}\right)\left(\frac{2}{-a^3}\right)+\frac{e^2B^2}{2mc^2}a-\frac{e^2}{2a^2}\cdot\frac{(1-\varepsilon)^{\frac{1}{2}}}{\varepsilon^{\frac{1}{2}}}\ln\left(\frac{1-\varepsilon^{\frac{1}{2}}}{1+\varepsilon^{\frac{1}{2}}}\right)=0 \quad (4.21)$$

and

$$\frac{\hbar^2}{2m}\cdot\frac{1}{3a^2}+\frac{e^2}{4a}\cdot\frac{1}{\varepsilon^{3/2}(1-\varepsilon)^{\frac{1}{2}}}\ln\left(\frac{1-\varepsilon^{\frac{1}{2}}}{1+\varepsilon^{\frac{1}{2}}}\right)+\frac{e^2}{2a}\cdot\frac{1}{\varepsilon(1-\varepsilon)^{\frac{1}{2}}}=0 \quad (4.22)$$

α_{11}, $\alpha_{\perp}$ and $\bar{\alpha}$ are then given by

$$\alpha_{11}=\frac{2e^2b^4}{Y-b^2X}$$

$$\alpha_{\perp}=\frac{2e^2a^4}{Z-a^2X} \quad (4.31)$$

$$\bar{\alpha}=(\alpha_{11}+2\alpha_{\perp})/3 \quad (4.5)$$

The numerical calculations based on these equations were carried out for InSb, taking

m = 0.01 x free electron mass

$\varepsilon_o = 16$

Equations (4.21) and (4.22) give a and ε (and hence b) as functions of B; X, Y and Z can then be computed and hence α_{11}, $\alpha_{\perp}$ and $\bar{\alpha}$ are

known, also as functions of B. The results of these calculations are shown graphically.

Fig. 6 shows the parameters a and b as functions of B.

Fig. 7 shows the function $\frac{4\pi}{3\varepsilon_o} N\bar{\alpha}$ as a function of B for different values of the impurity concentration, N.

Fig. 8 shows $\frac{4\pi}{3\varepsilon_o} N\alpha_{\parallel}$ and $\frac{4\pi}{3\varepsilon_o} N\alpha_{\perp}$ as functions of B for a fixed value of N ($N = 10^{16}$ cm^{-3}).

4.6 Discussion and Conclusions.

The results of the present calculation are shown in Figs. 6, 7 and 8.

Fig. 6 shows that the geometrical parameters a and b, characterizing the spatial distribution of charge around the impurity in the directions perpendicular and parallel to the magnetic field, respectively, both decrease as B increases, a decreasing more rapidly than b. This is in agreement with the result of Yafet, Keyes and Adams (Ref. 6) shown in Fig. 1, as is to be expected.

Fig. 7 has been drawn with our dielectric criterion for conduction in the impurity band, equation (4.2) in mind. In the region above the horizontal dashed line, the system is conducting; below this line it is non-conducting. We see that for an impurity concentration of, for example, 10^{16} cm^{-3}, the system is non-conducting for magnetic fields greater than 25,000 gauss. It is tempting to compare this result with the calculation of Fenton and Haering (Ref. 5) shown in Fig. 3, where for an impurity concentration of 5.7×10^{15} cm^{-3} a reduction in the number of conduction electrons occurs at a field of about 20,000 gauss. Fenton and Haering, however, are concerned with a Mott transition in which screening of the impurities by conduction electrons plays a vital role, while our calculation does not discuss such screening and is concerned with a transition taking place entirely within the impurity band. The two models here give critical fields

which do not differ greatly; we shall see below that there are experimental results which agree closely with the predictions of Fenton and Haering.

Fenton and Haering have calculated that for impurity concentrations greater than a critical value ($\sim 10^{14}$ cm^{-3}) there will be no bound states of the impurity. The results of our calculation (Fig. 7) suggest that there will be no conduction in the impurity band below this concentration, even in zero magnetic field.

Before turning our attention to the experimental work which has been done we question whether our method of averaging the polarizabilities α_{11} and $\alpha_{\perp}$ to obtain $\bar{\alpha}$ is appropriate. In an experimental situation the experimenter may decide to apply his magnetic field in a direction perpendicular (or parallel) to his electric field; it does not necessarily follow that he should then use only $\alpha_{\perp}$ (or α_{11}) in comparing theory and experiment. In order to decide how $\alpha_{\perp}$ and α_{11} should be combined a fuller discussion, involving the dependence of α on the direction of the wave-vector $\underset{\sim}{k}$, might be called for; some work on these lines has been done by Lobo, Rodriguez and Robinson (Ref. 16). Fig. 8 shows, for N = 10^{16} cm^{-3}, that the critical fields in the extreme cases, using only α_{11} or only $\alpha_{\perp}$, differ by an order of magnitude. It is surprising, therefore, that Putley (Ref. 18) found that rotating the magnetic field from the transverse to the parallel direction produced little effect.

Hanley and Rhoderick (Ref. 17) have carried out Hall effect measurements on n-type InSb with excess donor concentrations of 3×10^{13} cm^{-3} and 2×10^{14} cm^{-3}, respectively below and above the critical concentration. Fig. 10 shows the Hall coefficient plotted against reciprocal temperature over a range of magnetic fields for both specimens. From the presence of maxima in these curves the authors deduce that two types of carrier take part in the conduction process and analyze their results on a two-band model. On this basis they give the following expression for the Hall coefficient, R:

$$R = \frac{R_0(1+x)(1+xb^{*2})}{(1+xb^*)^2} \qquad (4.33)$$

where $x = n_c/n_i$; $b^* = \mu_c/\mu_i$;

$$R_0 = \frac{1}{e(n_i+n_c)} = \frac{1}{e(N_D-N_A)}$$

In this notation n is the electron concentration, μ the mobility, N_D the donor impurity concentration, N_A the acceptor impurity concentration and the subscripts c and i denote conduction band and impurity band, respectively. The authors assume that b^* varies more slowly with temperature than x and deduce that the maximum

value of R, which occurs when $x = 1/b^*$, is given by

$$R_{max} = \frac{R_0(1+b^*)^2}{4\,b^*} \qquad (4.34)$$

We now point out that when the magnetic field, B, increases the width of the impurity band decreases and consequently the effective mass, m_i^*, of an electron in the impurity band increases. Since μ_i is inversely dependent on m_i^* (page 194 of Ref. 4) the result of increasing B is to increase $b^*(=\mu_c/\mu_i)$. The result of increasing B is therefore to increase R_{max}, as the curves of Fig. 10 show. The present thesis suggests that above a critical value of B the impurity band is non-conducting; this may be interpreted by saying that at the critical field μ_i becomes zero and the value of b^* becomes very large. To see whether this is indeed so we examine the numerical results of Hanley and Rhoderick given in Table 3 (below), in which E_{theor} is the ionization energy predicted by Fenton and Haering (Ref. 5) and E_{exp} is the ionization energy deduced by Hanley and Rhoderick from their measurements. The measured and predicted values of ionization energy are also shown in Fig. 11 together with the prediction of Yafet, Keyes and Adams (Ref. 6) for an isolated hydrogen-like impurity.

We note, from Table 3, that the value of b^* does increase rapidly with magnetic field, particularly for the purer specimen, in which an increase of magnetic field from 6.25 kG to 43.75 kG (by a

Table 3

γ	5·2	10·4	15·6	20·8	26·0	31·2	36·5	
H(kG)	6·25	12·5	18·75	25·0	31·25	37·5	43·75	
$E_{theor}(\mathscr{R}^*)$	2·1	2·6	3·1	3·5	3·8	—	4·1	Specimen (A)
$E_{exp}(\mathscr{R}^*)$	1·8	2·1	2·6	3·3	4·0	—	4·4	$N_D - N_A = 3 \times 10^{13}$ cm^{-3}
N_A(cm^{-3})	9×10^{13}	1×10^{14}	2×10^{14}	$5{\cdot}5 \times 10^{14}$	6×10^{14}	—	7×10^{14}	$\mu(4{\cdot}2\ ^\circ\text{K}) = 1{\cdot}3 \times 10^5$ cm^2 V^{-1} s^{-1}
$b^* = \mu_c/\mu_1$	4·3	12·8	25·6	66·5	118	—	626	
$E_{theor}(\mathscr{R}^*)$	0·85	1·35	1·75	2·20	—	2·90	—	Specimen (B)
$E_{exp}(\mathscr{R}^*)$	0·8	1·6	2·0	2·4	—	2·9	—	$N_D - N_A = 2 \times 10^{14}$ cm^{-3}
N_A(cm^{-3})	4×10^{13}	6×10^{14}	2×10^{15}	9×10^{15}	—	1×10^{16}	—	$\mu(4{\cdot}2\ ^\circ\text{K}) = 1 \times 10^5$ cm^2 V^{-1} s^{-1}
$b^* = \mu_c/\mu_1$	2·8	10·0	24·5	41·2	—	75·4	—	

factor of 7) results in an increase of b* by a factor of 150. It should be pointed out, however, that the results shown in Table 3 are for magnetic fields greater than the critical field according to our calculations; nevertheless, there is qualitative support for our idea that increasing the magnetic field beyond a certain value cuts off the conduction process in the impurity band. Turning our attention to the predicted and measured values of ionization energy (Fig. 11) there is good agreement between experiment and the theory of Fenton and Haering, particularly for the less pure specimen and particularly for low magnetic fields. Hanley and Rhoderick state that their values of ionization energy have a precision of about 20%; at the higher magnetic fields used this could mean that their results are not far below the theoretical values of Yafet, Keyes and Adams (Ref. 6) for an isolated impurity. In fact, Durkan, Elliott and March (Ref. 19) predict that at high magnetic fields the ionization energy should approach the values of Yafet, Keyes and Adams and this is verified by the work of Beckman, Hanamura and Neuringer (Ref. 15) who found that with samples of impurity concentrations 2.6×10^{15} cm^{-3}, 3.7×10^{15} cm^{-3} and 1.1×10^{16} cm^{-3} the values of the ionization energy approached the theoretical values of Yafet *et al.* very closely at fields greater than 50 kG.

Hanley and Rhoderick's results are also consistent with the theory of Fenton and Haering in that they find zero ionization

energy for impurity concentrations greater than the critical value and a finite ionization energy at concentrations less than this. Hanley and Rhoderick also point out, in a note at the end of their paper (Ref. 17), that the activation energies predicted by Durkan and March are smaller than those observed by Hanley and Rhoderick and suggest that this may be due to the excited states of the impurity not playing the part envisaged by Durkan and March.

The work of Beckman, Hanamura and Neuringer (Ref. 15) mentioned above was carried out on impure samples at magnetic fields up to 150 kG. They found that below a critical magnetic field there was zero ionization energy but for fields greater than this the Hall coefficient and the transverse magnetoresistance both increased rapidly. This is in qualitative agreement with our theory, though their critical fields are larger (by a factor of 5 for a sample with impurity concentration $\sim 10^{16}$ cm^{-3}). They also deduce a relationship between the critical field and the impurity concentration which agrees closely with a similar relationship which may be derived from our results (Fig. 7) as follows.

We note first that if B is sufficiently large the curves of Fig. 7 all have the same slope, s (a negative number), which can be calculated. Since Fig. 7 is a log-log plot it follows that for a fixed value of N

$$\overline{\alpha} \propto B^{s} \qquad (4.35)$$

The critical values of $\bar{\alpha}$ and B are therefore related by

$$\alpha_c \propto B_c^{\,s} \tag{4.36}$$

Now $\bar{\alpha}_c$ is related to N by our conduction criterion, namely

$$\frac{4\pi}{3\varepsilon_0} N\bar{\alpha}_c = 1$$

$$\bar{\alpha}_c \propto N^{-1} \tag{4.37}$$

Hence, from (4.36),

$$B_c^{\,s} \propto N^{-1}$$

$$B_c \propto N^{-1/s} \tag{4.38}$$

This gives, from Fig. 7 (or, more readily, from the computed values of $\bar{\alpha}$ as a function of B)

$$B_c \propto N^{0.90} \tag{4.39}$$

This is close to the relationship quoted by Beckman, Hanamura and Neuringer (Ref. 15):

$$B_c \propto N^{6/7} = N^{0.86} \tag{4.40}$$

Finally, we refer to the work of Putley (Ref. 18) on a sample of InSb with an excess electron concentration of 5×10^{13} cm^{-3}, lower than the critical concentration. He found the existence of a non-zero activation energy for magnetic fields greater than a critical value; above this value the Hall coefficient increased with B. Putley's results have been interpreted by Durkan, Elliott and March (Ref. 19) in terms of a transition within the impurity band from a conducting to a non-conducting state at the threshold magnetic field; this is precisely the transition with which the calculations of the present thesis have been concerned. In fact, as March points out in the discussion at the end of Ref. 19, there are two mechanisms at work in reducing the conductivity when the magnetic field is increased: the Wigner transition, involving a decrease in the overlap between impurity states, to which we have applied the dielectric theory of the present work, and the Mott transition depending on the screening of the impurity states by conduction electrons, discussed by Fenton and Haering (Ref. 5).

In conclusion, then, we note that the dielectric approach to impurity conduction yields a critical value of the magnetic field at which the Wigner transition occurs. Our model is restricted by the assumption that $T = 0^{o}K$, so that the effects of screening by conduction electrons and of excited states of the impurities are neglected. Nevertheless our calculations agree with the results of

Beckman, Hanamura and Neuringer (Ref. 15) particularly with respect to the dependence of the critical field on impurity concentration and are in qualitative agreement with the work of Hanley and Rhoderick (Ref. 17), particularly with respect to the rapid increase of the ratio μ_c/μ_i with magnetic field. The latter's results support the calculations of Fenton and Haering (Ref. 5) with regard to activation energies.

References

1. Mott, N.F., 1956, Can. J. Phys., 34, 1356-1368.

2. Schiff, L.I., 1955, "Quantum Mechanics", 2nd Ed., (New York: McGraw-Hill).

3. Kittel, C., 1966, "Introduction to Solid State Physics", 3rd Ed., (New York: Wiley).

4. Ziman, J.M., 1965, "Principles of the Theory of Solids", (Cambridge: University Press).

5. Fenton, F.W. and Haering, R.R., 1967, Phys. Rev., 159, 593-599.

6. Yafet, Y., Keyes, R.W. and Adams, E.N., 1956, J. Phys. Chem. Solids, 1, 137-142.

7. Keyes, R.W. and Sladek, R.J., 1956, J. Phys. Chem. Solids, 1, 143-145.

8. Durkan, J. and March, N.H., 1968, J. Phys. C., 1, 1118-1127.

9. Hebborn, J.E. and March, N.H., 1964, Proc. R. Soc., A, 280, 85-96.

10. Durkan, J., Hebborn, J.E. and March, N.H., 1965, Proc. Int. Conf. Magn., Nottingham, 1964, (London: Institute of Physics and Physical Society).

11. Wallis, R.F. and Bowlden, H.J., 1958, J. Phys. Chem. Solids, 7, 78-89.

12. Frood, D.G.H., 1959, Proc. Phys. Soc., 75, 2, 185-193.

13. Condon, E. and Shortley, G., 1951, "The Theory of Atomic Spectra", (Cambridge: University Press).

14. Fröhlich, H., 1958, "Theory of Dielectrics", (Oxford: Clarendon Press).

15. Beckman, O., Hanamura, E. and Neuringer, L.J., 1967, Phys. Rev. Letters, 18, 19, 773-775.

16. Lobo, R., Rodriguez, S. and Robinson, J.E., 1967, Phys. Rev., 161, 2, 513-525.

17. Hanley, P.E. and Rhoderick, E.H., 1969, J. Phys. C., 2, 365-371.

18. Putley, E.H., 1961, J. Phys. Chem. Solids, 22, 241-247.

19. Durkan, J., Elliott, R.J. and March, N.H., 1968, Rev. Mod. Phys., 40, 812-815.

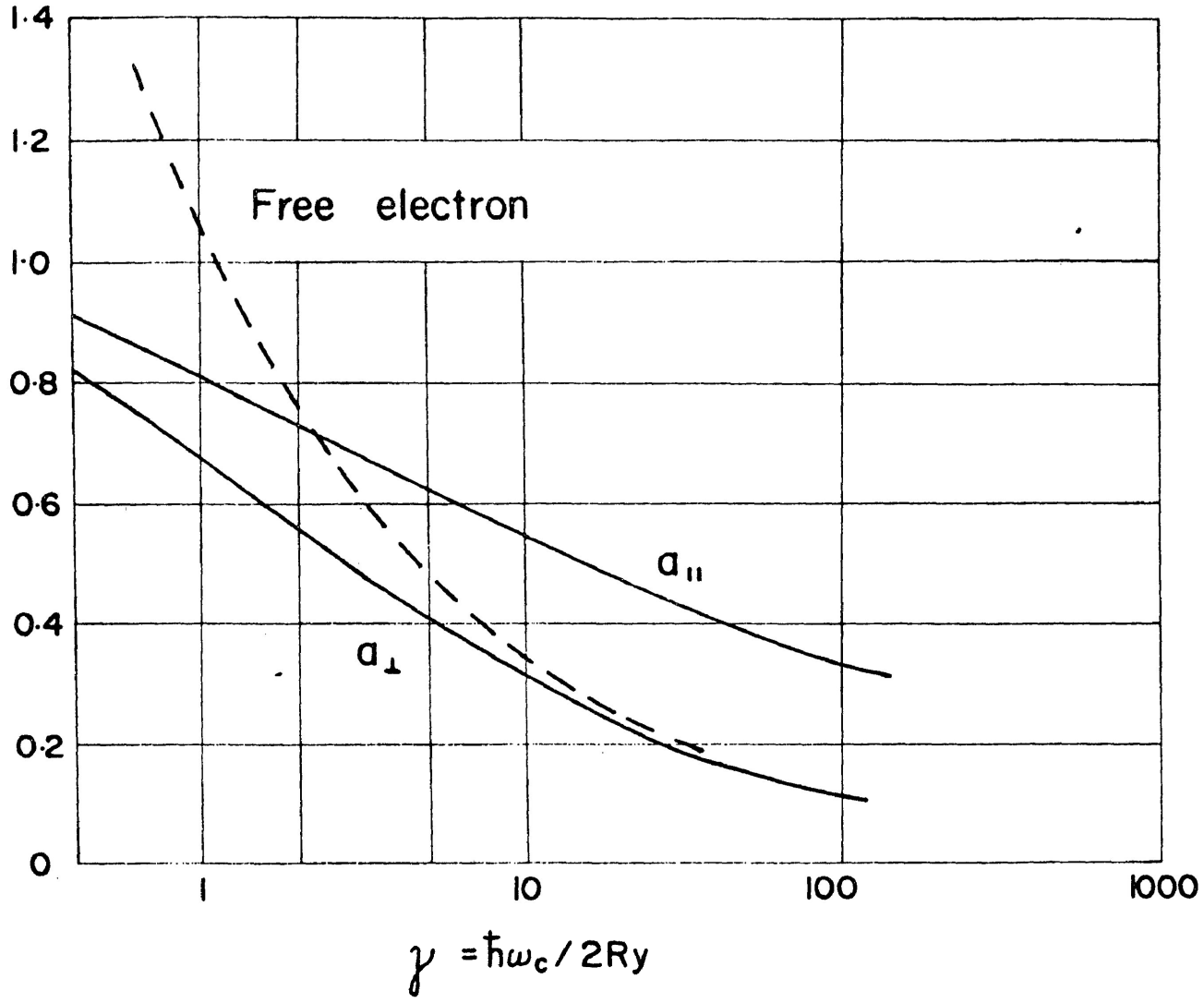

Figure 1

Impurity Charge Distribution as a Function of Magnetic Field - from Yafet, Keyes and Adams (Ref. 6).

$a_{\perp}$ and $a_{\parallel}$ (identical with our a, b) measure the ground state distribution from the impurity center in directions transverse and parallel to the magnetic field, respectively. γ is a dimensionless measure of magnetic field strength, B; for *InSb*, $B = 1.2$ *kG* when $\gamma = 1$. The unit of length (y-axis) is the best value of $a_{\perp}$ and $a_{\parallel}$ in zero magnetic field. The dashed curve shows the distribution for a free electron.

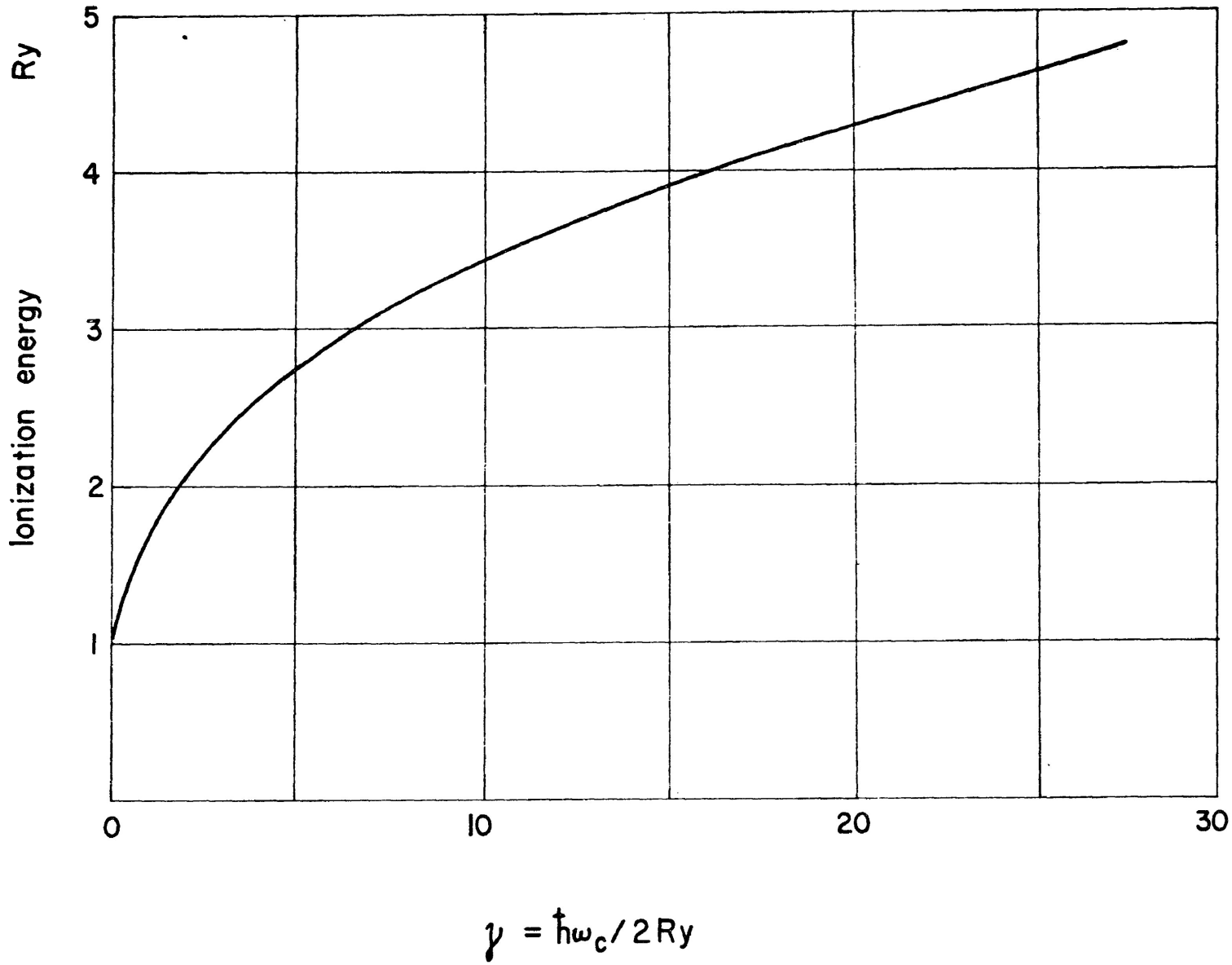

Figure 2

Ionization Energy as a Function of Magnetic Field - from Yafet, Keyes and Adams (Ref. 6).

γ is a dimensionless measure of magnetic field strength, B; for *InSb*, $B = 1.2$ *kG* when $\gamma = 1$. The unit of energy is the Rydberg.

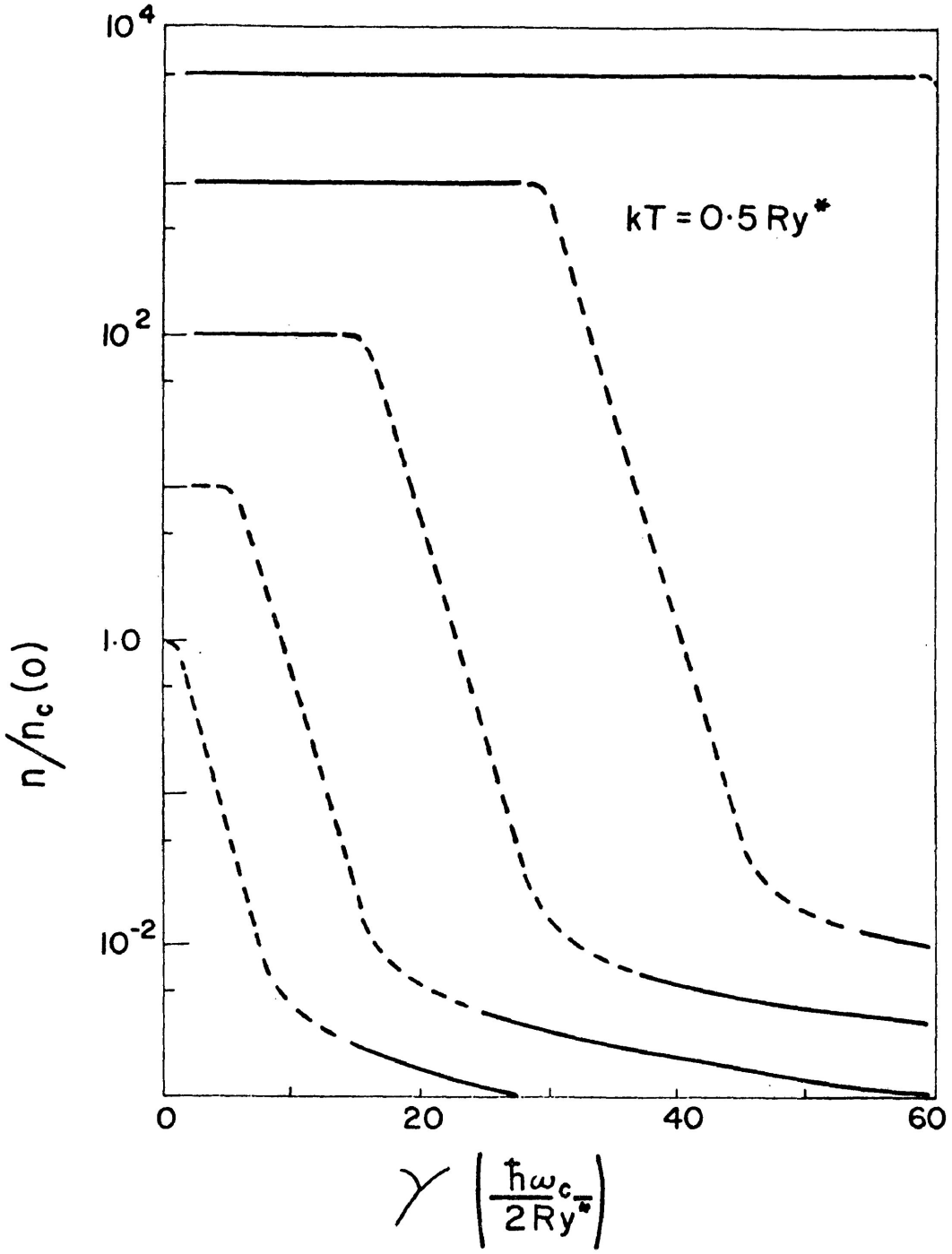

Figure 3

Conduction Electron Concentration as a Function of Magnetic Field - from Fenton and Haering (Ref. 5).

γ is a dimensionless measure of magnetic field strength, B; for *InSb*, $B = 1.2$ *kG* when $\gamma = 1$. n is the conduction electron concentration. For *InSb*, $n_c(0) = 5.7 \times 10^{13}$ cm^{-3} and *1 Ry* = 7.27°*K*. The impurity concentration is equal to the number of free electrons at zero field.

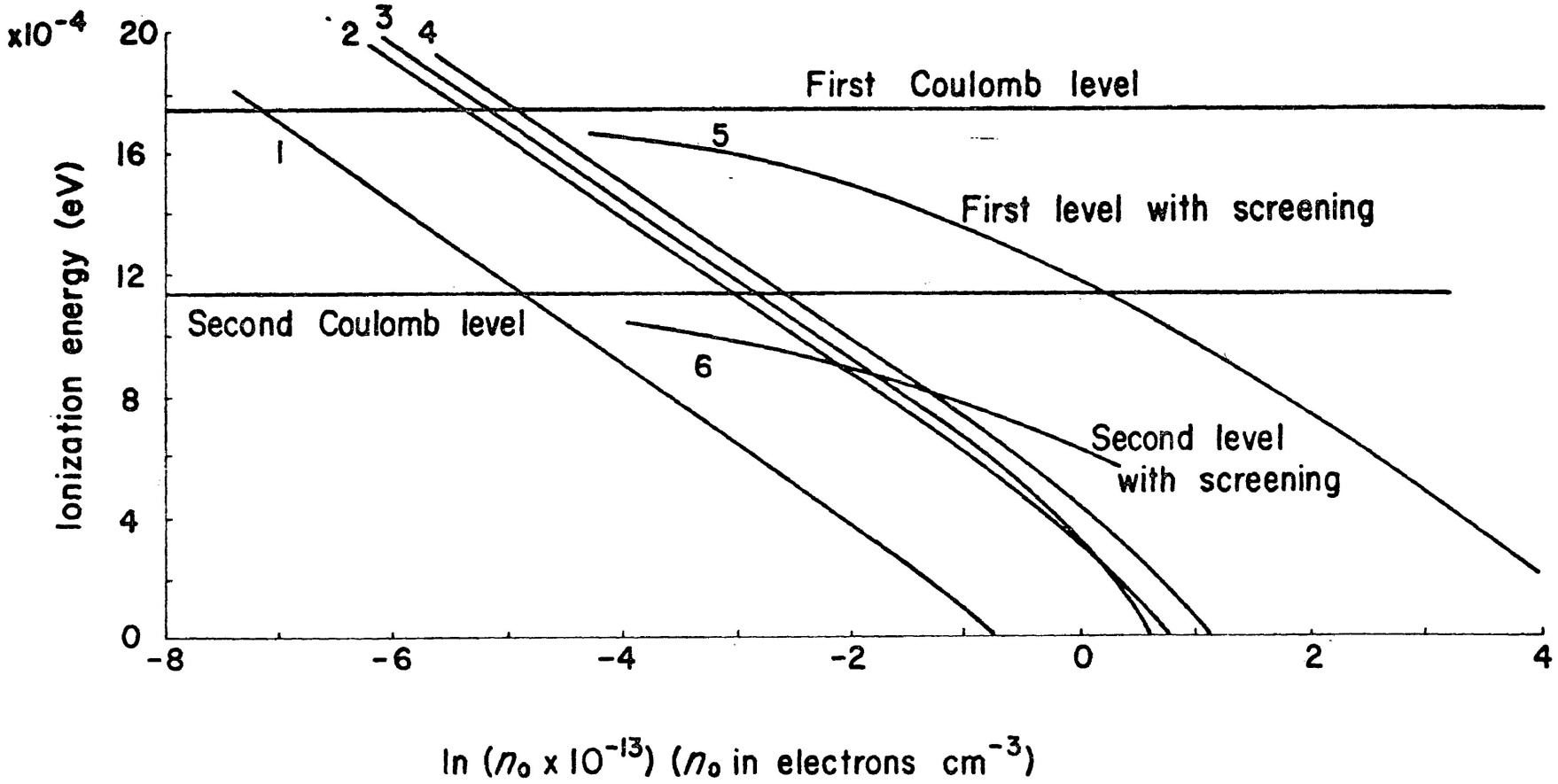

Figure 4

Ionization Energy as a Function of Conduction Electron Concentration - from Durkan and March (Ref. 8).

The data are shown for a magnetic field of 5 *kg* and a temperature of $3^{o}K$. Curves 1-4 refer to the samples described in the accompanying table. Curves for the first and second Coulomb level refer to the unscreened impurity. Where curves 5 and 6 intersect 1-4 we obtain ionization energies for the first and second levels with screening.

Sample	$N_d \times 10^{-13}$	$N_a \times 10^{-13}$
1	*100*	*98*
2	*43*	*38*
3	*24*	*21*
4	*45*	*38*

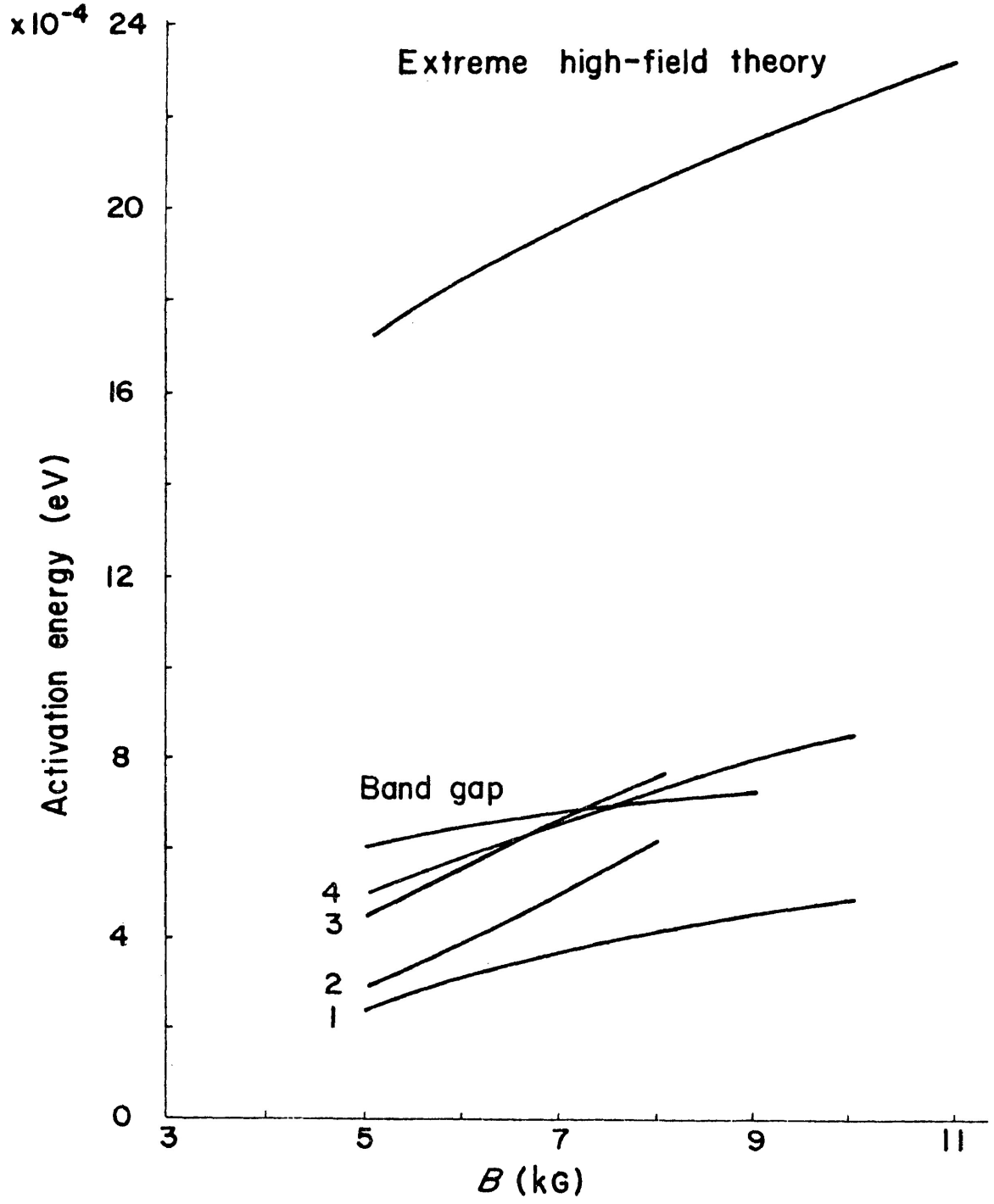

Figure 5

Activation Energy as a Function of Magnetic Field - from Durkan and March (Ref. 5).

Curves 1-4 represent the samples of Fig. 4. Curve labelled Band Gap is separation of lowest two impurity levels. Upper curve is the result of the theory of Yafet, Keyes and Adams (Ref. 6) for an isolated impurity.

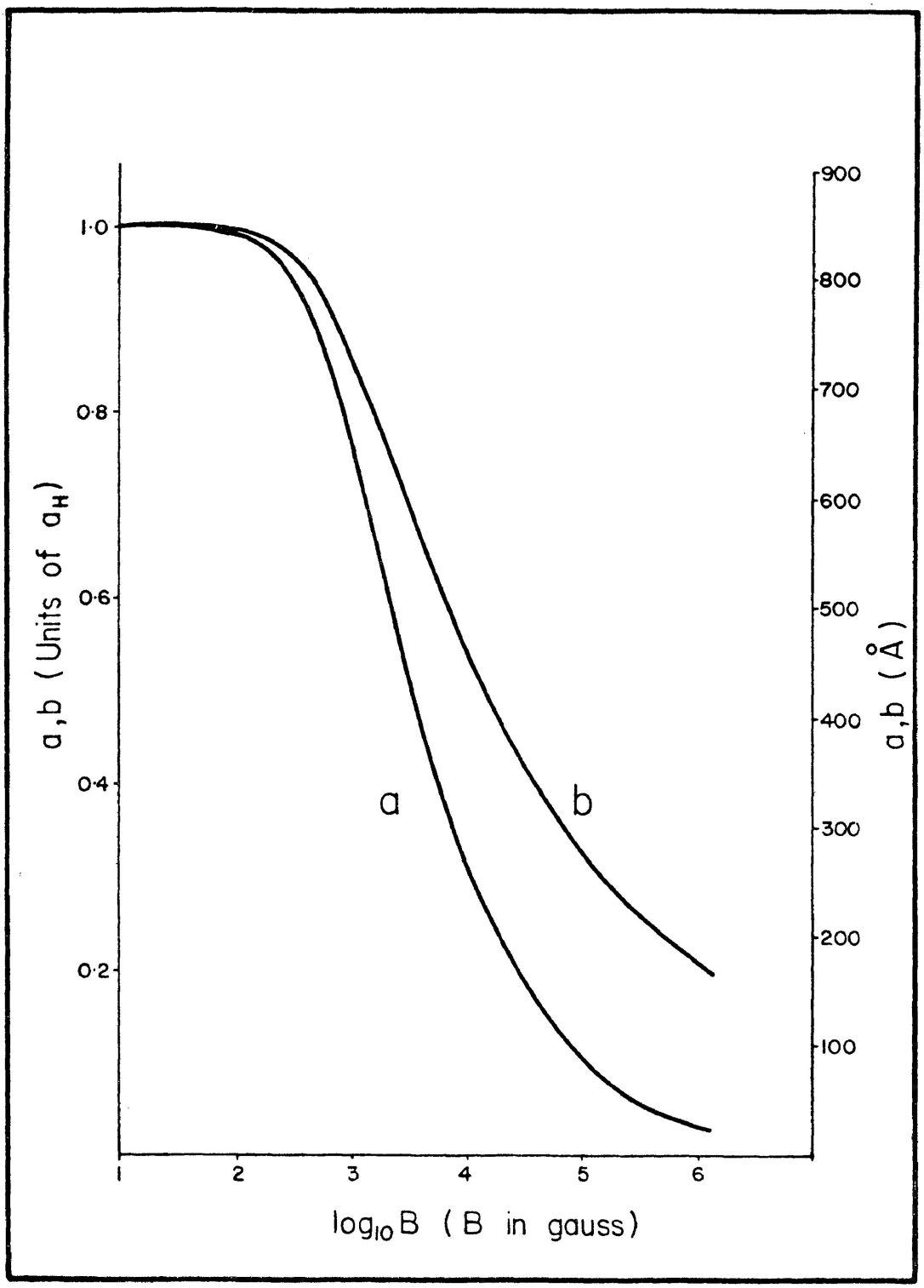

Figure 6

Impurity Charge Distribution as a Function of Magnetic Field - as calculated in this thesis.

a and b measure the ground state distribution from the impurity center in directions transverse and parallel to the magnetic field, respectively. a_H is the effective Bohr radius. The calculations are for *InSb*, taking the effective mass to be 0.01 × free electron mass and the background dielectric constant to be 16.

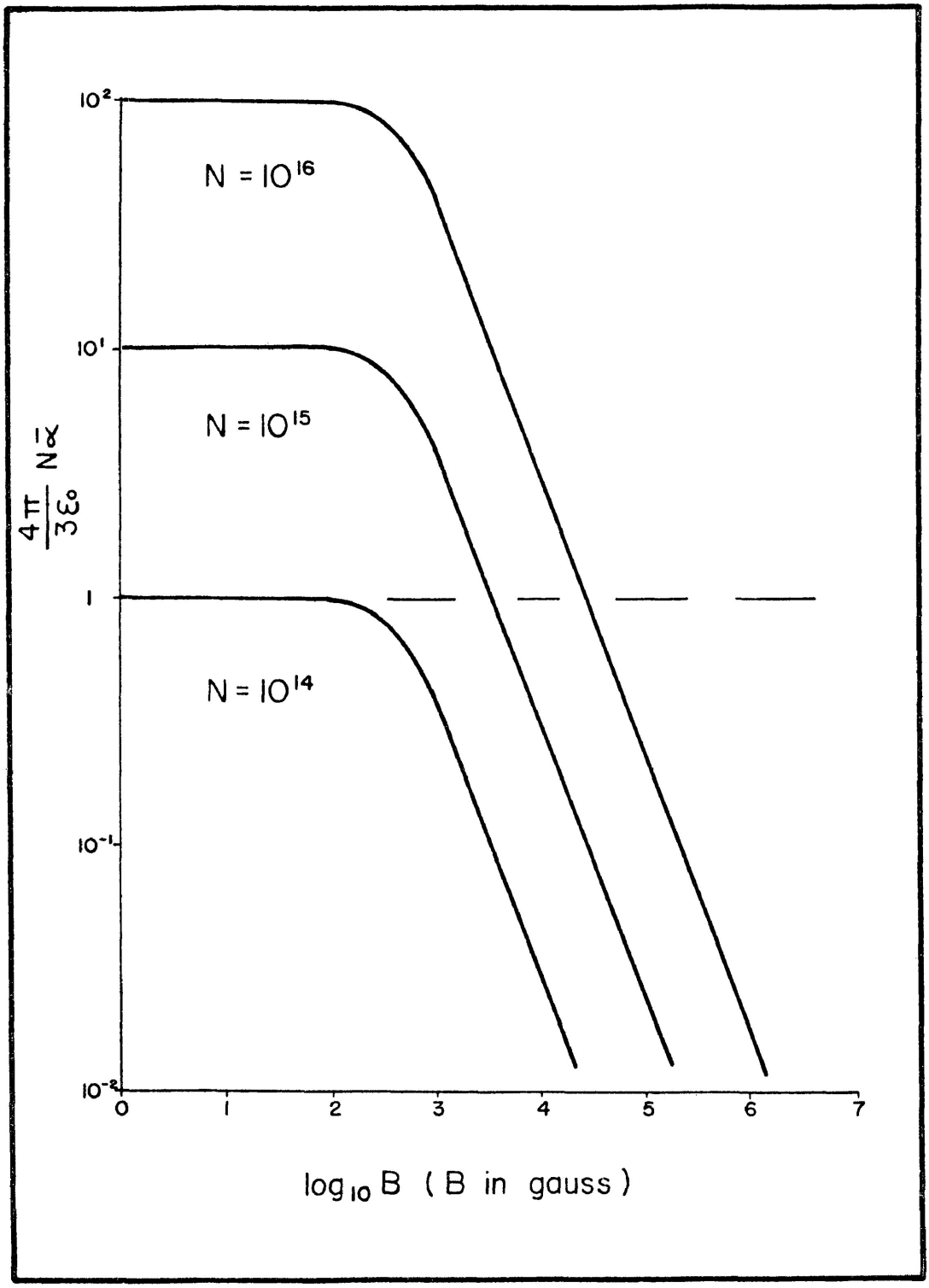

Figure 7

$4\pi N\bar{\alpha}/3\varepsilon_0$ as a function of B - as calculated in this thesis.

$\bar{\alpha}$ is average polarizability of an impurity in cm^3. N is donor concentration in cm^{-3}. The calculations are for *InSb*, taking the effective mass to be 0.01 × free electron mass and the background dielectric constant to be 16. The horizontal dashed line marks the boundary between regions in which impurity conduction does (above the line) and does not (below the line) take place.

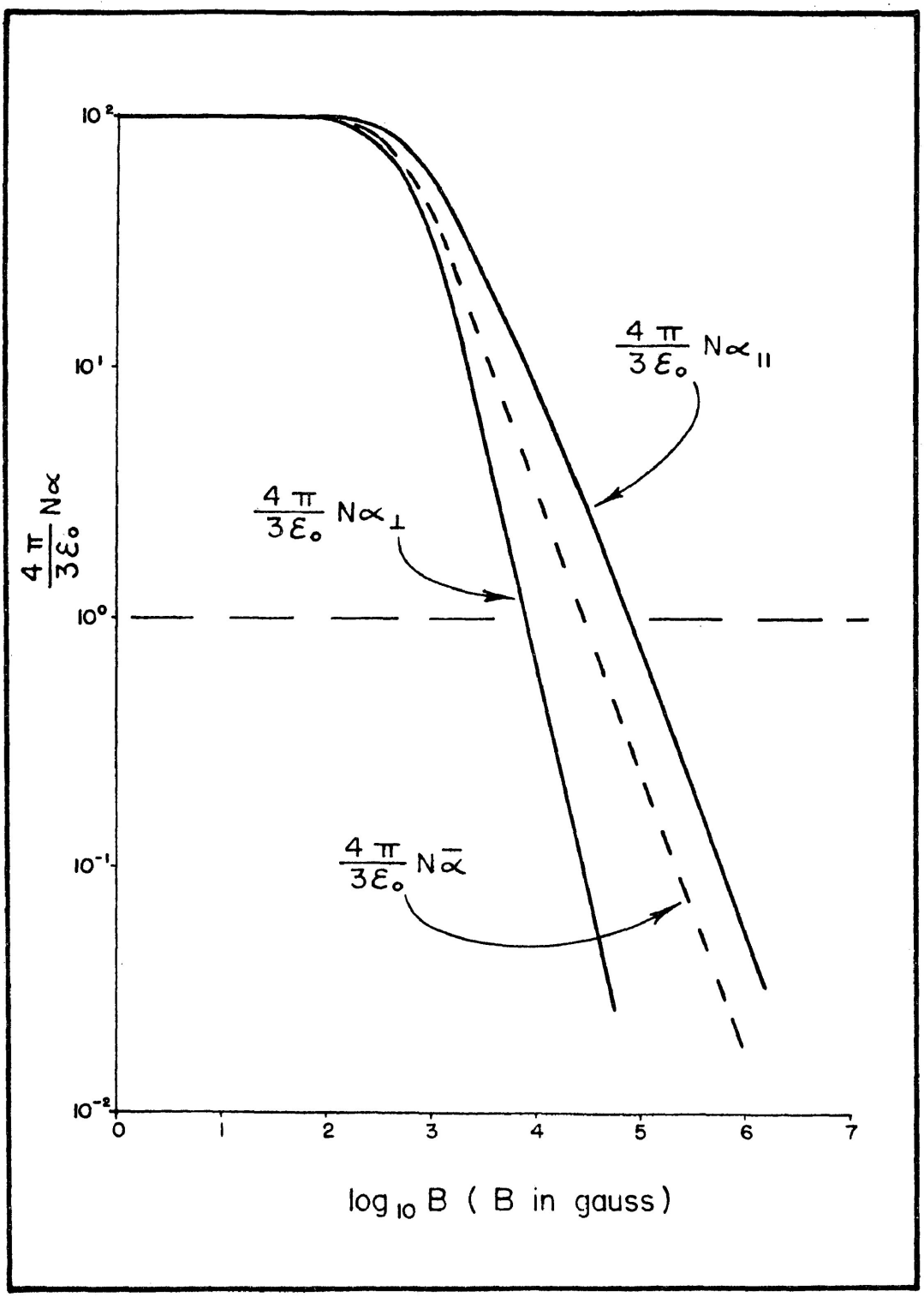

Figure 8

$4\pi N\alpha/3\varepsilon_0$ as a function of B - as calculated in this thesis.

The dashed curve reproduces the curve of Fig. 7 for $N = 10^{16}$ cm^{-3}. The full curves are for the extreme cases in which the magnetic field is perpendicular to ($\alpha_{\perp}$) or parallel to (α_{11}) the electric field. The critical field, where these curves cross the horizontal dashed line, differs by an order of magnitude in these extreme cases.

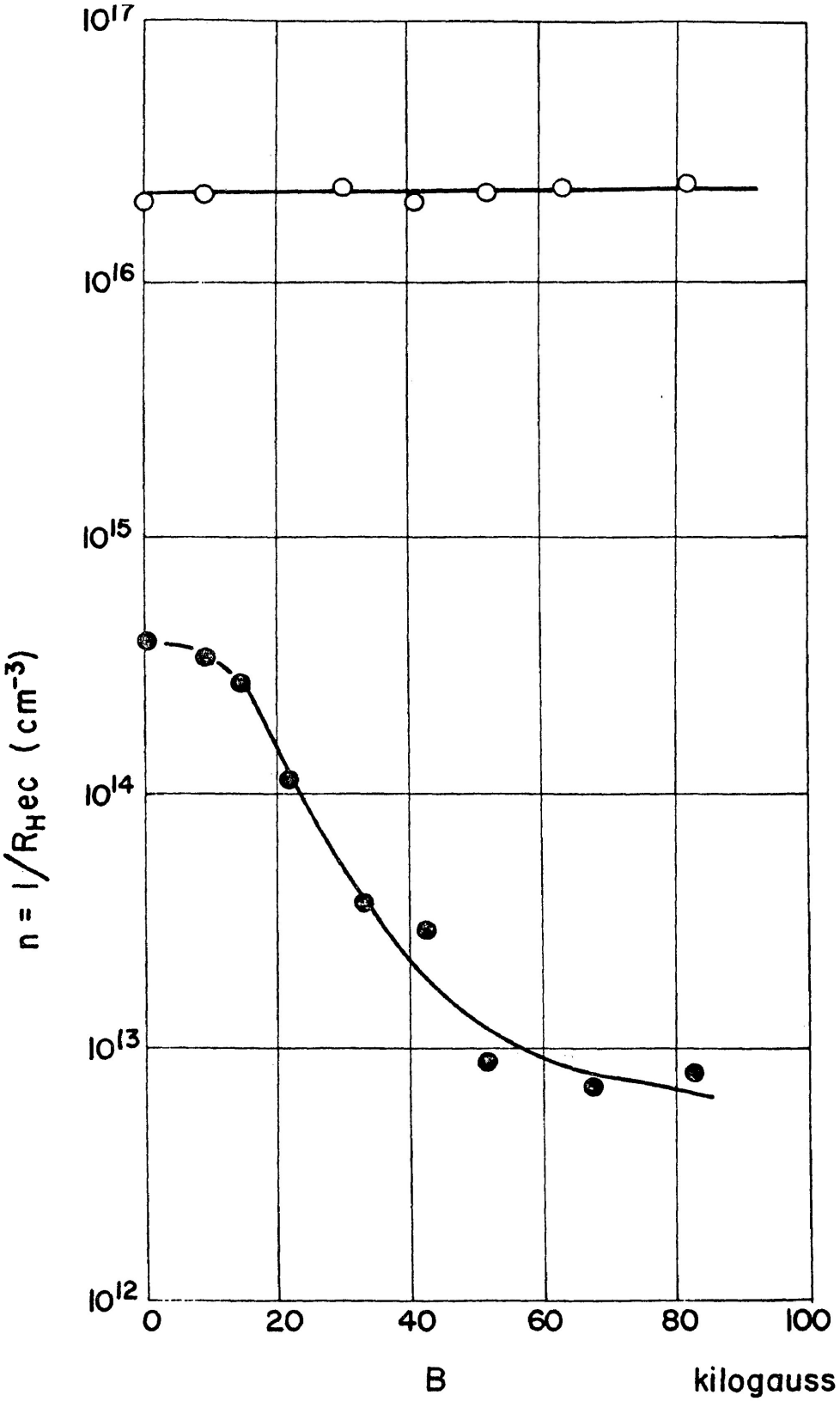

Figure 9

Conduction Electron Density as a Function of Magnetic Field - from Keyes and Sladek (Ref. 7).

n is the conduction electron density derived from Hall effect measurements at $4.2^{\circ}K$. The two curves are for samples with impurity concentrations of 10^{16} cm^{-3} (points marked ○) and 10^{14} cm^{-3} (points marked ●).

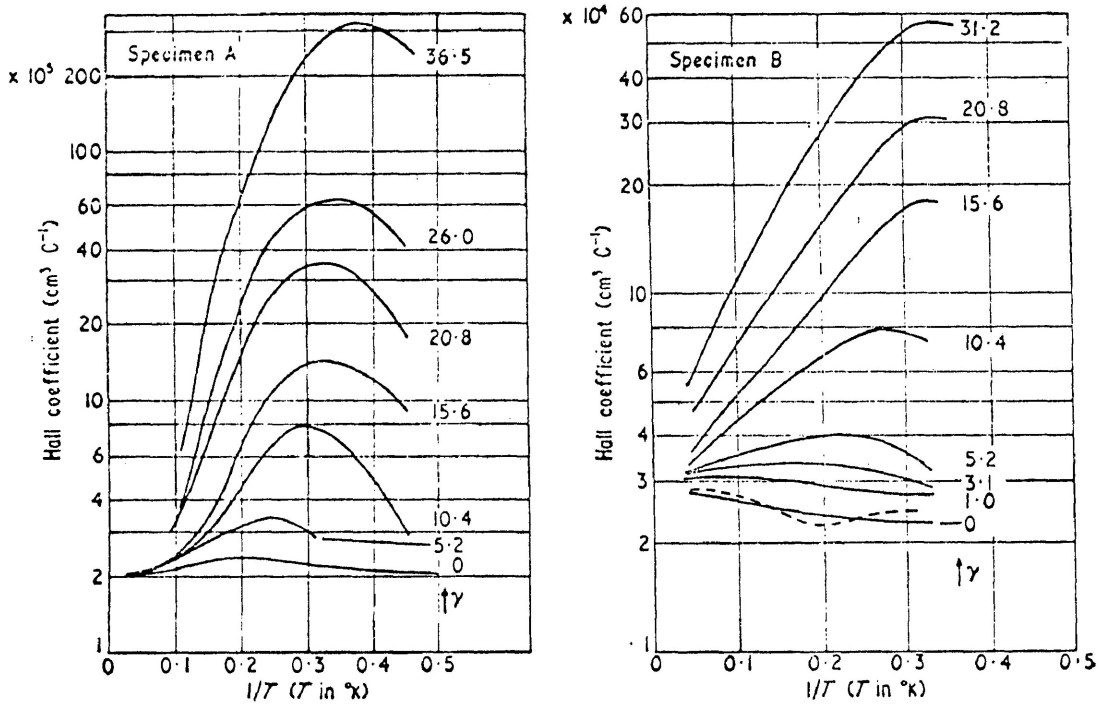

Figure 10

Hall Effect as a Function of Reciprocal Temperature - from Hanley and Rhoderick (Ref. 17).

Specimens *A* and *B* are *InSb* with excess donor concentrations of 3×10^{13} cm^{-3} and 2×10^{14} cm^{-3}, respectively. The curves are for different magnetic fields characterized by different values of the parameter Υ. For *InSb*, $B = 1.2$ *kG* when $\Upsilon = 1$. The broken curve for specimen *B* represents zero magnetic field measurements before etching.

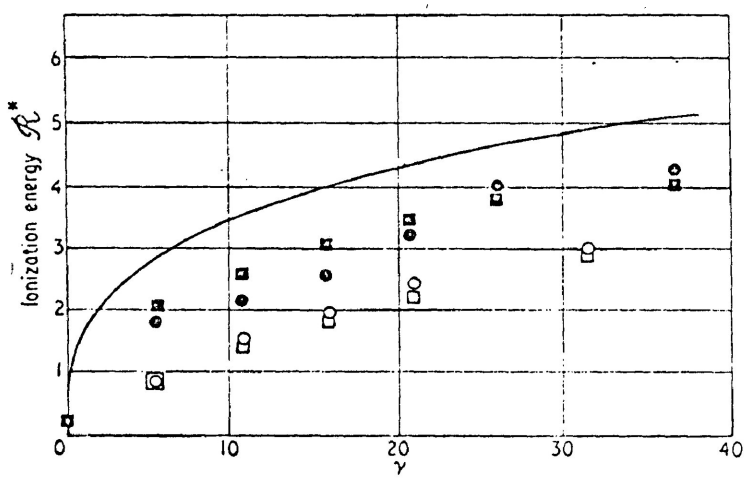

Figure 11

Ionization Energy in *InSb* as a Function of Magnetic Field - from Hanley and Rhoderick (Ref. 17).

γ is a measure of magnetic field; for *InSb*, $B = 1.2\ kG$ when $\gamma = 1$. The full curve is for an isolated impurity according to the theory of Yafet, Keyes and Adams (Ref. 6). The points shown are measured and predicted values for two specimens, *A* and *B:*

	N_D-N_A	*Measured*	*Predicted*
SPECIMEN *A*	$3\times10^{13}cm^{-3}$	●	■
SPECIMEN *B*	$2\times10^{14}cm^{-3}$	○	□

List of Symbols

a_H	Ground-state Bohr radius
e	Effective charge of an electron
m	Effective mass of an electron
$\hbar$	(Planck's constant)/2π
	1/(screening length)
ε_o	Static dielectric constant of background crystal
ε_s	Static dielectric constant of crystals plus impurities
ω_c	Cyclotron frequency
R_y	Rydberg
γ	$\hbar\omega_c/2R_y$
ϕ	Trial wave functions
p	Momentum of an electron
B	Magnetic field
β	Variational parameter

a	Variational parameter, radius perpendicular to B
b	Variational parameter, radius parallel to B
L_z	Angular momentum operator
d	a/b
E	Energy
v	Velocity of an electron
c	Velocity of light
ϵ	$1 - a^2/b^2$
H	Hamiltonian operator
n_o	Electron number density
k_B	Boltzmann's constant
T	Temperature
$\underset{\sim}{A}$	Magnetic vector potential
$\underset{\sim}{q}$	Electron wave vector
N	Impurity concentration
Na	Acceptor concentration

N_d	Donor Concentration
α	Polarizability
$\alpha_{\parallel}$, $\alpha_{\perp}$	Polarizabilities parallel or perpendicular to B
n	Principal quantum number
n'	Highest non-catastrophic quantum number
A_n	Population density of n-th energy level
A(T)	Number density of un-ionized donors
I_o	Ionization energy of ground-state
T_o	I_o/k_B
μ	Dipole moment of excited state
f	Local field
P	Polarization
F	Electric field (macroscopic)
F_c	Cavity field
g	Reaction field factor